Master of Science Thesis

Independent Monitor Unit Calculations in Intensity Modulated Radiotherapy

Helena Ramsing

Supervisors: Sven Bäck, Ph.D. and
Crister Ceberg, Ph.D.

Medical Radiation Physics
Clinical Sciences, Lund
Lund University, 2006

Abstract

Independent dose calculations in radiotherapy are important as they help assure that the dose given to the patient is the same as the prescribed. The current version of software Radiation Verification Programme, RVP, does not take into account the effects that occur when a beam from a linear accelerator is moved off-axis. The aim with this project was to find a model for these effects, fit the parameters in the model with data from measurements and then to test the model in clinically relevant situations. Preferably the model should be easily incorporated into the software.

Three variable parameters were used for the model; the slope, which is the proportional factor with which the dose increases with the distance, the width which affects the penumbra, and the leakage, which is the transmission through the field shielding. To fit the parameters for the model, measurements of fields placed off-axis were performed. This was done for two different linear accelerators; Varian Clinac 2100 and Elekta Precise, and one energy for both accelerators; 6 MV (Mega Voltage). Profiles were measured as to get the fields' entire spread. The data gained from these measurements were used to fit the model's parameters. The fitted model was first tested on profiles and then on IMRT fields in two dimensions.

The model was simple, both in terms of measurements and implementation and showed good agreement for profiles measured through the central axis. The second step was to test the model for IMRT fields. The 2D arrays were compared using gamma comparison and with a 5 %/5 mm demand the pass rate was very high. Only a small number of fields were used and therefore no statistical certainty is guaranteed, but if further testing get similar results, the model can be used in clinical cases for dose calculations for beams off-axis and IMRT fields.

ABSTRACT ..... **- 2 -**

1 INTRODUCTION ..... **- 4 -**

1.1 BACKGROUND ..... - 4 -
1.2 RECOMMENDATIONS FOR RADIOTHERAPY ..... - 5 -
1.3 THE IN-HOUSE DEVELOPED SOFTWARE, RVP ..... - 5 -
1.4 AIM ..... - 6 -

2 THEORY ..... **- 7 -**

2.1 THE CALCULATION MODEL ..... - 7 -
2.1.1 Adjustment of the model's parameters ..... *- 9 -*
2.1.2 Test of the model ..... *- 9 -*
2.1.3 Off-axis Softening ..... *- 10 -*
2.2 GAMMA EVALUATION ..... - 10 -

3 MATERIAL AND METHODS ..... **- 11 -**

3.1 OFF-AXIS MEASUREMENTS ..... - 11 -
3.1.1 The Linear Accelerators ..... *- 11 -*
3.1.2 The Acquiring of Data ..... *- 11 -*
3.1.3 Blue Phantom ..... *- 11 -*
3.1.4 LDA-99, Linear Diode Array ..... *- 11 -*
3.1.5 Measurements ..... *- 11 -*
3.2 OPTIMISATION ..... - 12 -
3.3 MEASUREMENTS FOR IMRT FIELDS ..... - 13 -
3.3.1 Treatment ..... *- 13 -*
3.3.2 The Linear Accelerator ..... *- 13 -*
3.3.3 The Detector System ..... *- 13 -*
3.3.4 Measurements ..... *- 14 -*
3.3.5 Comparison of IMRT fields with RVP ..... *- 14 -*

4 RESULTS AND DISCUSSION ..... **- 15 -**

4.1 OFF-AXIS MEASUREMENTS ..... - 15 -
4.1.1 Varian Accelerator ..... *- 15 -*
4.1.2 Elekta accelerator ..... *- 17 -*
4.2 OPTIMISATION ..... - 18 -
4.2.1 Varian Accelerator ..... *- 19 -*
4.2.2 Elekta Accelerator ..... *- 21 -*
4.3 IMRT MEASUREMENTS ..... - 23 -

5 CONCLUSIONS ..... **- 26 -**

6 ACKNOWLEDGEMENTS ..... **- 27 -**

7 SUMMARY FOR THE GENERAL PUBLIC (IN SWEDISH) ..... **- 28 -**

8 REFERENCES ..... **- 29 -**

8.1 ARTICLES ..... - 29 -

9 APPENDICES ..... **- 32 -**

9.1 APPENDIX 1, LIST OF ABBREVIATIONS ..... - 32 -
9.2 APPENDIX 2 ..... - 33 -
9.3 APPENDIX 3, CALCULATED, MEASURED AND GAMMA MATRICES ..... - 36 -

1 Introduction

1.1 Background

This Master's Thesis Project was carried out at the radiotherapy departments of Lund University Hospital and Malmö University Hospital.

In Sweden approximately 50 000 patients a year are diagnosed with some sort of cancer [SOS]. Worldwide, it is estimated that the cancer incidence is circa 40 %. This number has increased due to an increase in the life expectancy [ICRP]. New treatment methods are repeatedly being developed, introduced clinically and further improve the chances of curing cancer.

Depending on the type of cancer different treatment methods are being used. The three most common methods are surgery, chemotherapy and radiotherapy. These methods can be used individually or in combination with each other. It is estimated that roughly one third of all patients with cancer will receive some sort of radiotherapy during their treatment; either as a curative treatment, as an adjuvant treatment or with palliative purposes [The Swedish Cancer Society].

Many improvements within radiotherapy have been made as a consequence of new imaging techniques. The most important imaging modalities are CT (Computed tomography), MRI (Magnetic Resonance Imaging), PET (Positron Emission tomography)and PET/CT. With these modalities it is possible to get a better outline of the tumour's spread as well as more accurate definitions of the organs at risk [Svensson and Möller, 2003]. The new imaging modalities have set new demands on radiotherapy, but have also given the opportunities to generate a better, more conformal treatment.

One of the most revolutionary ideas within radiotherapy development was that of Intensity Modulated Radiation Therapy, IMRT, proposed in 1982 by Brahme [Svensson and Möller, 2003]. By modulating the intensity of the beam the flexibility increases and this can be utilised to achieve a higher degree of spatial agreement of the resulting dose distribution within the tumour [Bortfeld, 2006]. Also, the surrounding tissue can be further spared. An IMRT treatment consists of several fields, each built up by segments of various shapes and sizes [Carlson, 2001]. As imaging techniques have been improved it has made it possible to implement IMRT into clinical treatments.

In the early days of IMRT the modulation was performed using compensation filters. These filters had many disadvantages; they had to be manufactured individually for each patient and they had to be switched within the treatment. Additionally a safety hazard was involved by handling these lead blocks above the patient. In the late 1980s the Multi Leaf Collimator (MLC) was introduced [Svensson and Möller, 2003]. The MLC was a great improvement to conventional radiotherapy but they also made IMRT more viable. The MLC consist of a large number of leaves. [Metcalfe *et.al*, 1997]. The leaves can move independently of each other and therefore it is possible to, rapidly, create the small irregular fields that build up an IMRT treatment. This makes the treatment faster and

more viable. There are different techniques for delivering an IMRT plan; sliding window and step-and-shoot. In the sliding window technique the MLC leaves are moving as the radiation is on, and by doing so, the intensity is modulated. In the step-and-shoot method each small segment is given and while the leaves change the radiation is off.

IMRT gives a more conformal therapy than conventional radiotherapy. However, there are many more steps in IMRT planning, which increases the risk of error. It is of importance that the delivered dose is accurate and that it is made sure that the delivered dose is the same as the prescribed dose.

1.2 Recommendations for Radiotherapy

All use of ionising radiation in Sweden is controlled by The Swedish Radiation Protection Authority (abbreviated as SSI). Clinical radiotherapy is controlled by two different constitutions from SSI, namely 2000:1, *Regulations on General Obligations in Medical and Dental Practices using Ionising Radiation*, and 2000:4, *Regulations on Radiation Therapy*.

There are two conditions that must be fulfilled for using ionising radiation in medicine. They are authorisation and optimisation. The definition of authorisation is that the collective gain for the patient, in terms of treatment and/or the possibilities to make a diagnosis is larger than any possible side effects from the exposure of radiation. The other criteria, optimisation, means, in terms of radiotherapy, that the dose plan should be adjusted in a way that the prescribed dose is achieved in the target and the radiation dose to healthy tissue is as low as is reasonably achievable.

As a step of their quality assurance recommendations IAEA (International Atomic Energy Aency) has suggested in vivo measurements as a step to ensure the delivered dose [IAEA report; *Quality Assurance of External Beam Radiotherapy*]. They recommend that in vivo dose measurements are performed before a treatment begins. This makes sure no errors have been made during the course of the treatment planning. Entrance dose measurements check the output, performance of the treatment apparatus and the accuracy of the patient set-up.

One of several important parameters in radiotherapy is the number of Monitor Units (MUs). Preferably the number of monitor units should be calculated using two independent methods, or at least two independent persons.

1.3 The In-house Developed Software, RVP

Previously a software application has been made that, independently of the TPS (Treatment Planning System), calculates the absorbed dose to the target during radiotherapy [Knöös *et.al* 2001; Johnsson, 2003]. The program, HandCalc, was implemented into handheld computers and has previously been in use at the radiotherapy department at the University Hospitals of Lund and Malmö. This program has since been developed and implemented into a PC program called Radiation Verification Programme

(RVP) [Nordström *et.al* 2005]. RVP is currently in use at four hospitals in Sweden and the same algorithms and methods are used in other sites around the world as well. An advantage is that the algorithm in RVP is not used in manual calculations or in those by the TPS.

However the programme does not take into account the effects that occur when the field is moved off-axis it calculates the same dose no matter of the position. In order to make the programme work for IMRT treatments these off-axis effects must be investigated. Each IMRT field is built up by several segments which are generally small, irregular and may be located off-axis. During IMRT treatments one point can be irradiated during one segment and have no irradiation during the next segment [Carlson, 2001]. Therefore the effects of what happens when the field is moved off-axis are important to investigate, since they are needed for a proper dose calculation. Not only will the application be useful for IMRT treatments, but its accuracy of calculating the dose for conventional fields will also be enhanced.

The model used for dealing with off-axis effects should be easy, which makes the process of implementing the programme simpler. Standard accelerator data and a few simple measurements is all that should be needed in order to implement the programme in clinical use.

1.4 Aim

The aim of this study is to modify the parameters in the existing algorithm in RVP, to address the issues raised in the recent development in radiotherapy, specifically IMRT.

The specific goal for the work within this thesis is to propose a simple method for head scatter, to fit model parameters to measurements and then to test the model in clinically relevant situations.

2 Theory

2.1 The Calculation Model

The current model in RVP is the following.

The construction on which the dose calculation model in RVP operates on is the following:

$$D = M \cdot \left(\frac{D}{M}\right)_{ref} \cdot \frac{T}{T_{ref}} \cdot \frac{K_P^{rel} \cdot \beta_P + K_{P,C}^{rel} \cdot \sigma}{\beta_{P,ref} + \sigma_{ref}} \qquad \text{Eq. 2.1}$$

Both T, an attenuation factor, and σ, the scatter-to-primary ratio are functions of the attenuation coefficient, μ [Bjärngard and Vadash, 1995]. T is also a function of the hardening coefficient η [Bjärngard and Shackford, 1994]. In this model, the electron equilibrium factor [Hannallah *et.al.* 1996] is not modelled but is set to $\beta_P = \beta_{P,ref} = 1$.

$K_{P,0}(field, \vec{r})$ is the primary kerma free in air. It is a function of the field shape and the position of the calculation point, $\vec{r} = (x, y, z)$, with isocentre at origo and the focal point of the radiation at (0;0;-f_{ref}). This gives the distance, f, from the focus to the calculation point as $f = \sqrt{x^2 + y^2 + (f_{ref} + z)^2}$

The reference kerma is set at a field size of 10x10 cm^2 and at the isocentre (**r**=0); $K_{P,0,ref} = K_{P,0}(10x10, \vec{r} = 0)$. By using the reference kerma $K_{P,0}$ can be related to a measurable quantity [Johnsson *et.al*, 1999],

$$K_P^{rel} = \frac{K_{P,0}}{K_{P,0,ref}} \qquad \text{Eq. 2.2}$$

For the scatter calculation (the second term in Equation 2.1), the strength of the source is represented by $K_{P,C}^{rel}$. In the previous version of RVP a very simple model for the primary kerma free in air was used, this model only took the inverse square law and the head-scatter according to;

$$K_P^{rel} = K_{P,C}^{rel} = \left(\frac{f_{ref}}{f}\right)^2 H(c_{eq}) \qquad \text{Eq. 2.3}$$

H is the head scatter contribution within the field and is a function of the equivalent field size at the isocentre (c_{eq}). In this model no consideration is taken to the variations in the fluency off-axis, the penumbra, the leakage outside of the field or the head-scatter contribution outside of the field. The aim of this work was to modify the model in order to take these effects into consideration. This was done by dividing the primary kerma free in air in one focal component and one extra focal component. The focal component is the

photons that come directly from the source while the extra focal photons have interacted in the accelerator head before reaching the patient or phantom.

$$K_{P,0} = K_{P,0}^{F} + K_{P,0}^{X} = \overbrace{a'_1 \left[\left(1 - L + S \cdot \sqrt{x_{iso}^2 + y_{iso}^2}\right) \cdot \Omega + L\right]}^{K_{P,0}^{F}} + \overbrace{a''_1 \left(1 - \exp\left(-a_2 \cdot c_{eq}\right)\right)}^{K_{P,0}^{X}} \qquad \text{Eq. 2.4}$$

Within the field the focal component is assumed to increase with the factor, S, as the calculation point is moved away from the isocentre. Outside of the field, the focal part decreases to the value L, the transmission through the field shielding. The parameter L only makes a difference when the calculation point is outside of the direct field, i.e. when $\Omega \neq 1$. The factor Ω is an error-function that describes the focal part's decreasing in the penumbra region according to;

$$\Omega = \frac{1 + erf\left(s \cdot W\right)}{2} \qquad \text{Eq. 2.5}$$

W is an adjustment parameter related to the focal size, and s is the shortest distance from (x_{iso}; y_{iso}) to the field's edge. s is positive if (x_{iso}; y_{iso}) is within the field and negative otherwise.

The extra focal part of the primary kerma free in air is supposed to be increasing with the equivalent field size, c_{eq}, according to an exponential function with the coefficient, a_2.The equivalent field size is calculated according to Xiao *et.al* (1999) and is then scaled to the isocentre distance;

$$c_{eq} = \left(f_{ref} \middle/ f \right) \cdot s_{eq}$$

This parameter has a value outside the field as well, which means that the extra focal component of the primary kerma also will reach outside the field.

The relationship between the focal and extra focal components are determined by the two factors, a_1' and a_1''. These factors include a decrease in accordance with the inverse square law. If a_1 is set to $a_1 = f^2 \cdot \left(a_1' / a_1''\right)$ the expression for K_P^{rel} becomes

$$K_P^{rel} = \left(\frac{f_{ref}}{f}\right)^2 \cdot \frac{a_1 \left[\left(1 - L + S \cdot \sqrt{x_{iso}^2 + y_{iso}^2}\right) \cdot \Omega + L\right] + \left(1 - \exp\left(-a_2 \cdot c_{eq}\right)\right)}{a_1 + \left(1 - \exp\left(-a_2 \cdot c_{eq}\right)\right)} \qquad \text{Eq. 2.6}$$

The denominator gets its more simple form due to the fact that $x_{iso}=y_{iso}=0$ and $\Omega=1$ in the reference situation.

The modified model is complemented by making the attenuation coefficient dependent on the off-axis position according to Tailor *et.al* (1998) (see section 2.1.3), for the calculation of T and σ. $K_{P,C}^{rel}$ is calculated for the point in the field in which c_{eq} is the largest, in this point it is for certain that $\Omega=1$ as there is no penumbra within the field.

2.1.1 Adjustment of the model's parameters

By adjusting the model to measurements done in the isocentre for square fields (f_{ref}=f, x_{iso}=y_{iso}=0 and Ω=1), the parameters a_1 and a_2, i.e. the field size dependence can be determined.

$$K_P^{rel} = \frac{a_1 + \left(1 + \exp\left(-a_2 \cdot c_{eq}\right)\right)}{a_1 + \left(1 + \exp\left(-a_2 \cdot c_{ref}\right)\right)} \qquad \text{Eq. 2.7}$$

The second step is determining the parameter L. This is done by adjusting the model for measurements at a distance outside of the field (f_{ref}=f, Ω=0)

$$K_P^{rel} = \frac{a_1 \cdot L + \left(1 + \exp\left(-a_2 \cdot c_{eq}\right)\right)}{a_1 + \left(1 + \exp\left(-a_2 \cdot c_{ref}\right)\right)} \qquad \text{Eq. 2.8}$$

The next step is to determine the fluence variation in off-axis positions, namely the parameter S. This is done by adjusting the model to measurements in various positions in the isocentre plane for the largest possible field size (f_{ref}=f, Ω=1)

$$K_P^{rel} = \frac{a_1 \cdot \left(1 + S \cdot \sqrt{x_{iso}^2 + y_{iso}^2}\right) + \left(1 + \exp\left(-a_2 \cdot c_{eq}\right)\right)}{a_1 + \left(1 + \exp\left(-a_2 \cdot c_{ref}\right)\right)} \qquad \text{Eq. 2.9}$$

In the final step, the variation of the primary kerma in the penumbra region is determined. The parameter W is determined by adjusting the model to measurements along the field edge in the reference field (f_{ref}=f)

$$K_P^{rel} = \frac{a_1 \cdot \left[\left(1 - L + S \cdot \sqrt{x_{iso}^2 + y_{iso}^2}\right) \cdot \Omega + L\right] + \left(1 + \exp\left(-a_2 \cdot c_{eq}\right)\right)}{a_1 + \left(1 + \exp\left(-a_2 \cdot c_{ref}\right)\right)} \qquad \text{Eq. 2.10}$$

2.1.2 Test of the model

The modified model is tested by comparisons to measurements done in the following situations:

i) Dose profiles in the isocentre plane at a 10 cm depth. The field sizes used were 3x3 cm^2, 5x5 cm^2 and 10x10 cm^2. The fields are placed symmetrically around the central axis or with an off-axis distance of ±5 cm or ±10 cm

ii) Dose matrices (2D) in the isocentre plane at a depth of 10 cm for clinically relevant IMRT fields

2.1.3 Off-axis Softening

The use of an attenuation correction suggested by Tailor *et.al* (1998) was also implemented. Since the flattening filter is cone shaped, fields that are off-axis will have a lower average energy, i.e. a higher share of low-energy photons [Metcalfe *et.al* 1997], for a large field this is known as the horns. The suggested way of dealing with this effect is to use a different attenuation coefficient, μ', in stead of μ, due to the passage through the flattening filter [Tailor *et.al* 1998]. μ' can be derived from the angle between the central ray and the ray through the calculation point.

$$\mu' = \mu \cdot \left[1 + 0.00181 \cdot \theta + 0.00202 \cdot \theta^2 - 0.0000942 \cdot \theta^3\right] \qquad \text{Eq. 2.11}$$

Where θ is given by

$$\theta = \arctan\left(\frac{\sqrt{x_{iso}^2 + y_{iso}^2}}{100}\right) \qquad \text{Eq. 2.12}$$

where x_{iso} and y_{iso} are the coordinates of the calculation point in the plane of the isocentre (as above)

2.2 Gamma Evaluation

In order to compare the measured and calculated matrices, a gamma evaluation is performed. Gamma evaluation can be used for comparison of 2D matrices of dose distributions. These matrices could be measured or calculated, as in this case, or it could be the distribution from the TPS. The measurements are used as reference and the other matrix is queried for comparison [Low *et.al* 1998]. When doing a gamma comparison two criteria are set, one for the dose and one for the distance.

The gamma method uses a combination of dose difference and distance to agreement (DTA) distribution to determine the acceptability of the dose calculation. The dose difference uses the dose criterion directly while the DTA is the distance between two points that displays the same dose, and the DTA and the dose-difference evaluations complement each other [Low *et.al* 1998]. If both the parameters of the criteria, dose and distance, pass or fail for a certain point no further more evaluations are made. If one parameter fails but the other is well within the criteria the calculation can still pass since both parameters are taken into consideration [OmniPro ImRT Manual].

3 Material and Methods

The effects that occur when a field is moved off-axis were investigated. For this purpose a series of measurements were performed. Various field sizes and positions off-axis were used. The results were implemented into the scripts of the RVP from which the parameters for the model were derived.

3.1 Off-axis Measurements

3.1.1 The Linear Accelerators

The accelerators used for the measurements off-axis were a Varian Clinac 2100C and an Elekta Precise. Both installed and in clinical use at the radiotherapy department at Malmö University Hospital. The acceleration voltage used for both accelerators was 6 MV.

3.1.2 The Acquiring of Data

The detector system used for the off-axis measurements were a Linear Diode Array (LDA-99), manufactured by Scanditronix-Wellhöfer. The measurements were performed in a blue phantom, by the same company.

3.1.3 Blue Phantom

The Blue Phantom was used for the off-axis measurements. The advantages of the phantom are that it is easy to align under a linear accelerator and its computer software can move the detector, placed in the phantom, to any position within an accuracy of 0.1 mm [Scanditronix-Wellhöfer]. It is also compatible with the LDA. During the measurements the phantom was filled with deionised water.

3.1.4 LDA-99, Linear Diode Array

The LDA-99 consists of 99 diodes spaced by 5 mm, meaning that the detector can cover 49 cm in total and thereby give profiles of the beams, in one direction at the time [Scanditronix-Wellhöfer]. The LDA, when placed in the blue phantom, is computer-controlled and by doing multiple measurements with small movements in between the resolution can be as low as 1 mm. The LDA has the advantage that it can measure profiles and give a total view of the field's spread. The acquiring was performed with the help of the electrometer that belongs to the LDA and its software. The diodes have a direct response which facilitates the measurements.

3.1.5 Measurements

For the measurements the SSD (Source to Surface Distance) was 90 cm and the detector placed at 10 cm depth. The measurements were performed in a Blue Phantom, with deionised water.

Three different field sizes were used. The reference field, for both the measurements as well as the calculations, was the 10x10 cm^2 field. All future measurements and calculations were normalised to this field. The other field sizes used were 3x3 cm^2 and 5x5 cm^2. The decision was made to focus on smaller fields since the fields for IMRT generally are small.

For off-axis measurements on the Varian machine, five points were used in the y-direction; y=0 cm, y=±5 cm and y=±10 cm. The chosen points were in the centre of each field. Using solely the main jaws of the accelerator, the fields in the off-axis y-direction were created.

For the Elekta accelerator the same technique was used, with the difference that the off-axis measurements were performed in the x-direction. Just as with the Varian, this was due to the limitations of the machine. For the Elekta machine the fields were created with a combination of the MLC and the main jaws.

The central diode of the LDA was at the isocentre and the other detectors were placed on the main axis. Due to the length of the LDA full profiles could be acquired in the given direction and the fields, even when far off-axis, were always covered. The LDA was calibrated due to background radiation before using it.

The output doses for the accelerators were also controlled measured by an ion chamber´. This was done in order to see how good the LDA preformed in the off-axis output measurements. These measurements did not give all the data that is needed to fit the parameters, as it only gives information in one point, and since the ion chamber has a larger spread than the diodes it was not as good for point measurements either, particularly for the smaller fields.

3.2 Optimisation

After the off-axis softening correction by Tailor *et.al* (1998) was incorporated into the script as the first correction, the real optimisation could begin. For the optimisation of the width and the leakage the reference field was used. For the slope optimisation two alternative data sets were used. The first consisted of all the fields (10x10 cm^2, 5x5 cm^2 and3x3 cm^2) for which the centre point of each field was used. The other data set consisted of points taken from the measurements of the 40x40 cm^2 field. The points used were located at every 2.5 cm from y=0 to y=10 cm.

It is assumed that the differences in dose output are the same in the x- and y-directions. For a complete implementation it would be necessary to perform measurements in both directions.

The optimisation was performed within Matlab. All relevant calculation points and their respective geometries were entered into a vector in Matlab. The dose per MU was calculated for every element and then compared with the measured values in the same

points. All three parameters' values were then found, in order, by searching for the minimum of the square sum of the difference between the calculated and measured values. This was done element by element and the value that returned the lowest value was set.

3.3 Measurements for IMRT fields

To truly test the model, measurements of an IMRT treatment were performed and then compared with calculations of the same treatment made by RVP.

3.3.1 Treatment

The IMRT treatment used was an actual IMRT treatment for a patient treated for tonsil cancer. This particular treatment consisted of seven fields, built up by a various number of segments. The number of segments in the various fields are presented in Table 3.1.

Table 3.1 The numbers of segments for the IMRT fields

Field number	Number of segments
1	28
2	24
3	28
4	24
5	30
6	26
7	38

3.3.2 The Linear Accelerator

The accelerator used for these measurements was the Elekta Precise, installed at Malmö University Hospital, for which off-axis measurements had been performed and parameters for the model had been derived.

3.3.3 The Detector System

The detector system that was used for the measurements of the IMRT fields was an IMRT-dedicated system, IMRTlog, manufactured by OncoLog Medical Systems. It is a 2D-array system and consists of 506 semiconductor detectors. The distance between the detectors is 10 mm and they are placed in a polystyrene phantom, on a depth of 0.5 cm, providing build-up, also additional build-up plastic plates of various thicknesses are provided. In addition, the system also has a fixed backscatter block [OncoLog; IMRTlog technical information].

The area of the detector plate is 21.0 cm times 22.0 cm (the number of detectors in each direction is 22 times 23), which means that, when centred, it reaches out to a point circa 10 cm off-axis. The way the 64 electrometers, and its associated ADC:s (Analogue to

Digital Converter), are assembled gives for 512 independent channels, and for each of these channels the dose resolution is better than 1 mGy [OncoLog, IMRTlog technical information]. The detector system has its own computer software that offers direct display of the dose and dose rate and also various means of displaying the results.

3.3.4 Measurements

The phantom with the detectors was placed with the centre detector at the isocentre. Calibration was performed before the actual measurements; by doing this the detector and its software were correctly oriented in the beam geometry. An output measurement for the 10x10 cm^2 field was also performed in order to perform output normalisation. RVP also performs output normalisation within its calculations. Ten cm of build-up was used for the measurements; 0.5 cm built-in polystyrene and 9.5 cm solid water (Gammex fabrication). Solid water is plates that are made to represent the properties of water. Its density is 1.03 g/cm^3 and it absorbs and scatters photons as if it was water [Solid water Phantoms].

3.3.5 Comparison of IMRT fields with RVP

Both RVP and the measurements produced 2D-arrays as results. The results from the measurements were 2D-arrays that covered an area of 22 cm by 23 cm with a resolution of 1 cm. The results from RVP are 81 by 81 pixels with a resolution of 0.5 cm. Therefore the RVP covers a larger area and has better resolution. Before the comparison could be performed the two arrays for the same field had to be of the same size and resolution. First the RVP arrays were cut as to cover the same area as the measured arrays, then their resolution were decreased so that the measurements and the calculations had been performed in the same points. Comparison could then be performed as the size (22x23 pixels) and resolution (1cm) of the two matrices were the same.

Scanditronix-Wellhöfer has developed a software application for verification of IMRT treatments (Omnipro ImRT). This is done by comparing two 2D arrays, one reference matrix and the one to be evaluated. The programme was used to compare the two matrices, the calculated one and the measured one; the measured was set as the reference matrix. In order to properly compare the two matrices, gamma evaluation was used.

Two criteria were set for the gamma evaluation; dose difference and distance. The evaluation was done for two sets of criteria; 2 % and 2 mm and 5 % and 5 mm. The 2 %/2 mm criteria were chosen since this is the accuracy the TPS has showed in previous studies [Knöös *et.al.*1994]. However, since RVP is meant to be a secondary test of the dose it does not have to be as accurate and if RVP is off by 5 % and 5 mm it is still considered well, therefore these criteria were used as well. Gamma evaluation was then performed for both sets of criteria. The search distance was 15 mm, to avoid overlap.

4 Results and Discussion

The off-axis measurements were performed on both a Varian Clinac and an Elekta Precise. With the data gathered the optimisation of the parameters could be carried out. The model was then tested on measured profiles and the ultimate test was to test the model on clinically relevant IMRT fields.

4.1 Off-axis Measurements

The measurements were performed for three different field sizes, 3x3 cm^2, 5x5 cm^2 and 10x10 cm^2. All measurements were output normalised to the 10x10 cm^2-field on-axis.

4.1.1 Varian Accelerator

As expected by Metcalfe *et.al*, (1997) the output dose was higher off-axis than on-axis. This was true for all three field sizes.

The full profiles for the fields were overlapped with the 40x40 cm^2 field's profile. This was done in order to see whether or not the increase in output for the smaller fields is related to that of the larger field, i.e. if the slope for the large field could be used. If that slope would work, the implementation would be easier as this data already is registered for all machines and energies. In order to get an accurate view the 40x40 cm^2 field was multiplied with a factor to get agreement between the two centre points as the larger field has a higher output dose.

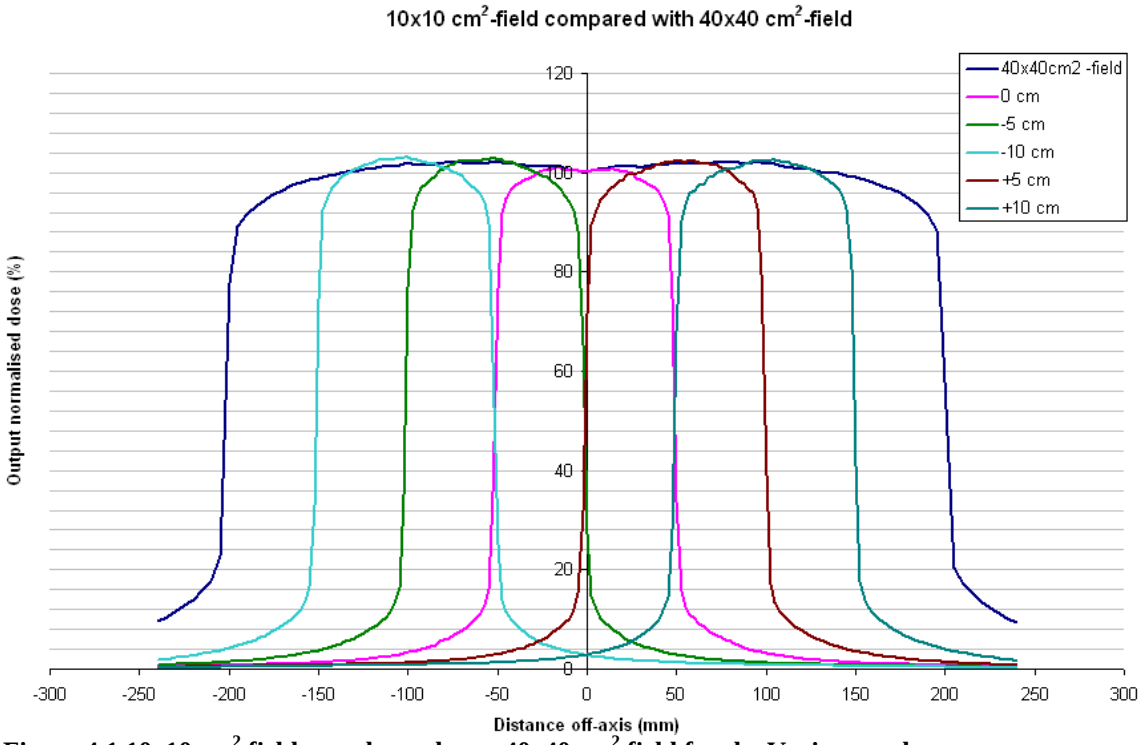

Figure 4.1 10x10 cm^2 fields overlapped on a 40x40 cm^2 field for the Varian accelerator

The 10x10 cm^2 fields and the large field are in good agreement (Figure 4.1), meaning that it could be possible to use the slope to model the off-axis change. The agreement is better on the positive side than on the negative side. The 5x5 cm^2-field and the 3x3 cm^2-field can be found in appendix 2.

For the smaller fields, the same tendencies are seen, the further away the beam got from the central axis the higher the dose was. The agreement between the largest field and the smaller fields was also good.

For the various field sizes on the Varian accelerator the output dose was higher on the negative side than on the positive side. This could be due to fluctuations in the accelerator or due to a slight misplacement of the LDA, thus getting a dose too high at the negative side and a dose too low at the positive side. Since values from both sides are used in the optimisation, these effects will cancel each other out. Even if the field is assumed to be symmetrical and the effects will cancel each other out, it gives a better outline to use points at both sides of the central axis.

Ion chamber measurements were conducted in order to validate the LDA for off-axis measurements. The deviations between the ion chamber and LDA for the different field size are presented in tables 4.1, 4.2 and 4.3.

Table 4.1 Deviations between ion chamber and LDA for 10x10 cm^2 field.

Off-axis distance	Deviation ion chamber vs. LDA (%)
-10	0.194
-5	0.487
0	0.398
+5	0.294
+10	0.784

Table 4.2 Deviations between ion chamber and LDA for 5x5 cm^2 field

Off-axis distance	Deviation ion chamber vs. LDA (%)
-10	0.194
-5	0.672
0	0.768
+5	0.653
+10	0.369

Table 4.3 Deviations between ion chamber and LDA for 3x3 cm^2 field

Off-axis distance	Deviation ion chamber vs. LDA (%)
-10	2.826
-5	3.248
0	2.745
+5	2.641
+10	2.567

The values for the smallest field deviate a lot since the spread of the ion chamber is as large as the field; therefore the values are not accurate. However it can be seen for the larger fields that the LDA and the ion chamber are close in values and this validates the measurements done by the LDA.

4.1.2 Elekta accelerator

The same tendencies were seen in the measurements at the Elekta accelerator as in the case of the Varian accelerator, the dose increases as the field is moved off-axis. The increase for this machine was not as high as for the Varian. This could be due to difference in the mounting of the jaws and also proves that machines from different brands do not have the same output, even if the energy is the same.

Also in this case the small profiles were compared with the largest field, 40x40 cm^2, to see if the horns of the output profile for the larger field could be used as the slope for off-axis corrections. The large field was also here multiplied with a factor to get agreement in the centre point.

For all fields the dose does follow the shape of the large field, but not entirely (Figure 4.2). The smaller fields can be seen in appendix 3.

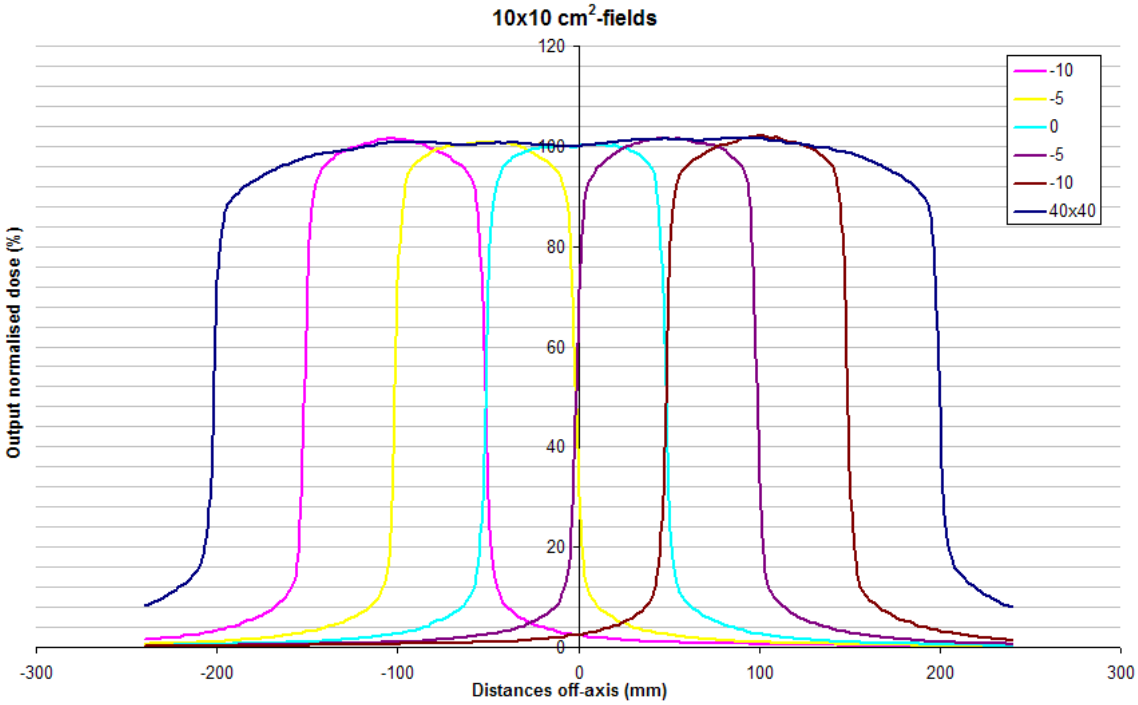

Figure 4.2 The 10x10 cm^2 fields overlapped on a 40x40 cm^2 field for the Elekta accelerator

While the agreement between the 10x10 cm^2-field and the 40x40 cm^2-field the two small fields, 5x5 cm^2 and 3x3 cm^2, did not follow the horns for the larger field. The increase for the Elekta accelerator is also lower than that for the Varian accelerator.

4.2 Optimisation

By the use of the measurements that had been performed the optimisation could take place. L and W were optimised using the 10x10 cm^2-field and two data sets were tested for the optimisation of S, the middle point of all small fields as well as points from the profile of the 4040 cm^2. Therefore only one value for L and W each will be provided and tested whereas two values will be tested for the slope, S.

When the small fields are used, the values for the parameter S are compromises between all field sizes. Therefore no field size or distance off-axis will get a perfect match, but on the other hand no field will get a match that is totally off.

The values derived from the optimisation were used to calculate the dose. The results from these calculations were then compared with the measured values. The deviations were calculated from the absolute values of the deviations, meaning that the average deviation does not indicate whether or not RVP over- or under-calculates the dose. For the calculation of the deviations the average of the points over 80% of the maximum value was used as those points were considered to be within the field without going out into the penumbra.

4.2.1 Varian Accelerator

The results of the optimisation of the Varian accelerator are presented in Table 4.4.

Table 4.4 The results of optimisation of S, W and L, Varian accelerator

	S	W	L
Small fields	0.0030	3.0931	0.0023
40x40 cm^2-field	0.0054	3.0931	0.0023

The slope derived from the small fields gave a good agreement between the calculated and the measured profiles (Figure 4.3). The deviations were generally small; the maximum deviation for all the calculated fields was less than 2%. The average, maximum and minimum deviations are presented in Table 4.5. All deviations are calculated as $\left|1-\frac{cal-meas}{cal}\right|$.

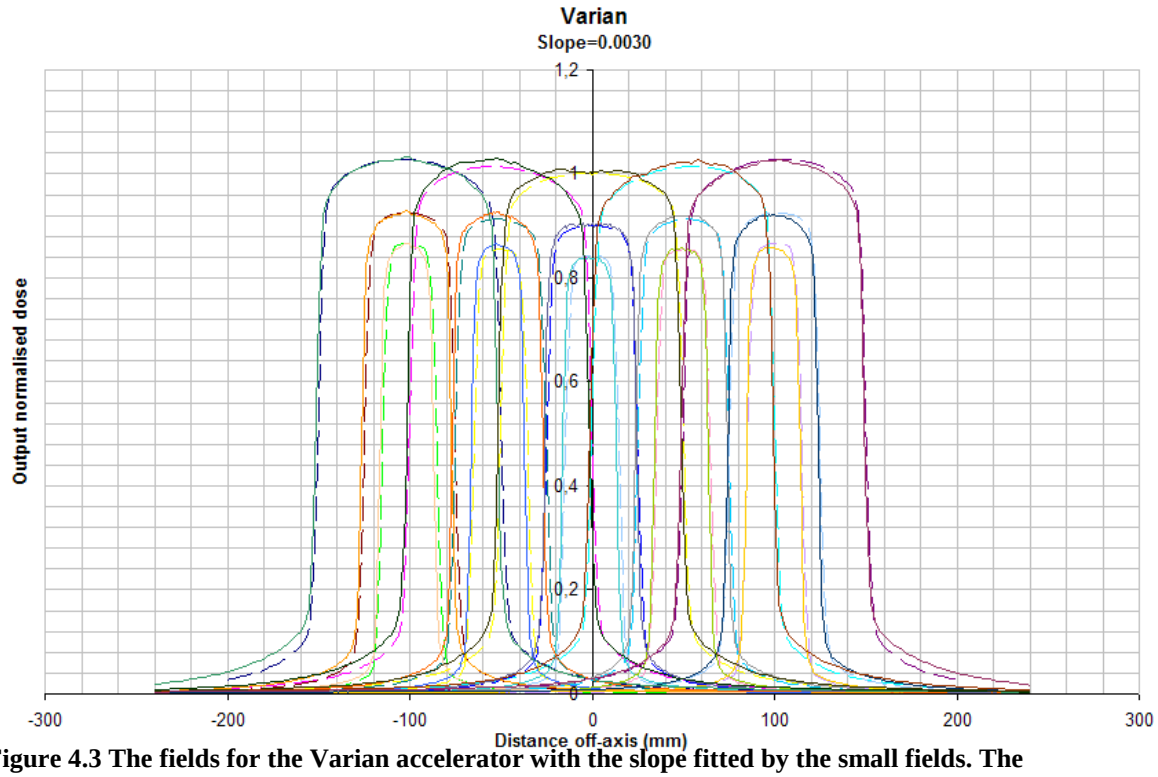

Figure 4.3 The fields for the Varian accelerator with the slope fitted by the small fields. The calculated values are dashed lines.

Table 4.5 Deviations (%) between RVP and the LDA for S=0.0030

Average deviation, 3x3 cm^2	0.81
Average deviation, 5x5 cm^2	0.61
Average deviation, 10x10 cm^2	0.58
Average deviation, all fields	0.67
Minimum deviation	0.05
Average minimum deviation	0.18

Maximum deviation	1.75
Average maximum deviation	1.17

The slope derived from the 40x40cm^2-field on the other hand was too high (Figure 4.4). For the field at the off-axis distance of 5 cm the agreement was still good, but the over-estimation by RVP at 10 cm was large.

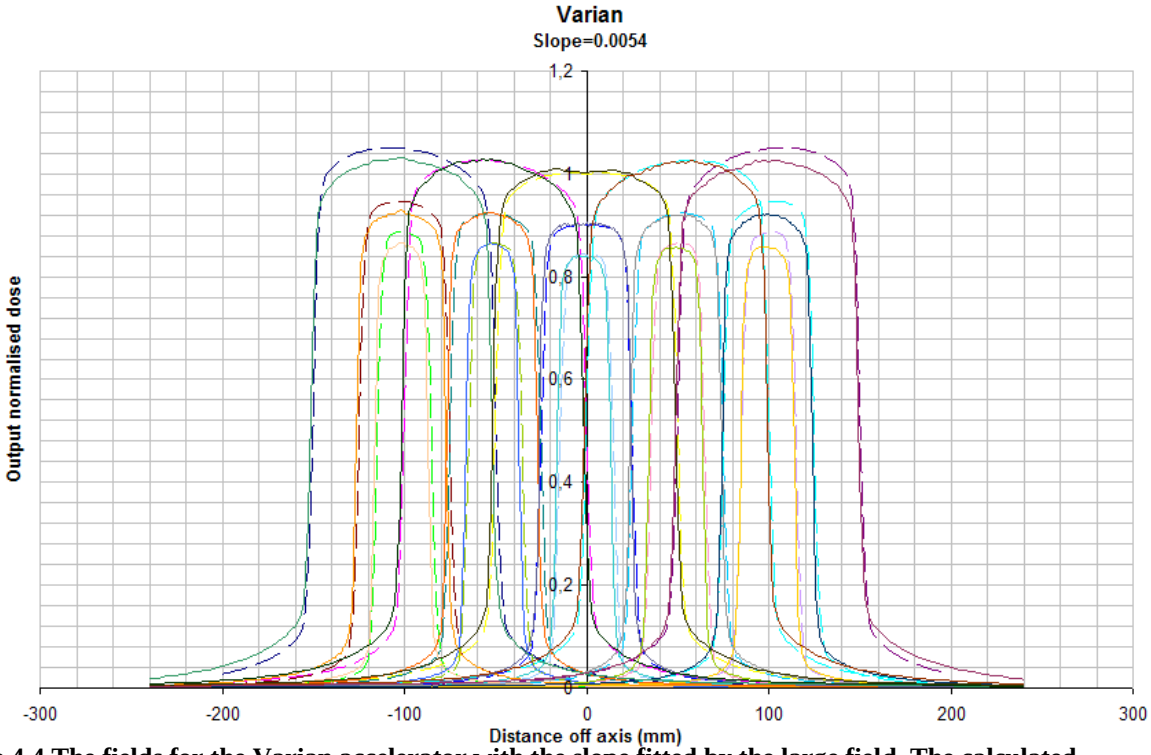

Figure 4.4 The fields for the Varian accelerator with the slope fitted by the large field. The calculated values are dashed lines.

The deviations found for this slope was also larger, no average deviation was lower than 1 % and the maximum deviations were high, all above 2.8 %, with the average maximum deviation at 3.37%.

Table 4.6 Deviations (%) between RVP and the LDA for S=0.0054

Average deviation, 3x3 cm^2	1.83
Average deviation, 5x5 cm^2	1.32
Average deviation, 10x10 cm^2	1.36
Average deviation, all fields	1.50
Minimum deviation	0.16
Average minimum deviation	0.27
Maximum deviation	4.03
Average maximum deviation	3.37

4.2.2 Elekta Accelerator

Table 4.7 The results of the optimisation of S, W and L, Elekta accelerator

	S	W	L
Small fields	0.0014	2.13	0.0079
40x40 cm^2-field	0.0038	2.13	0.0079

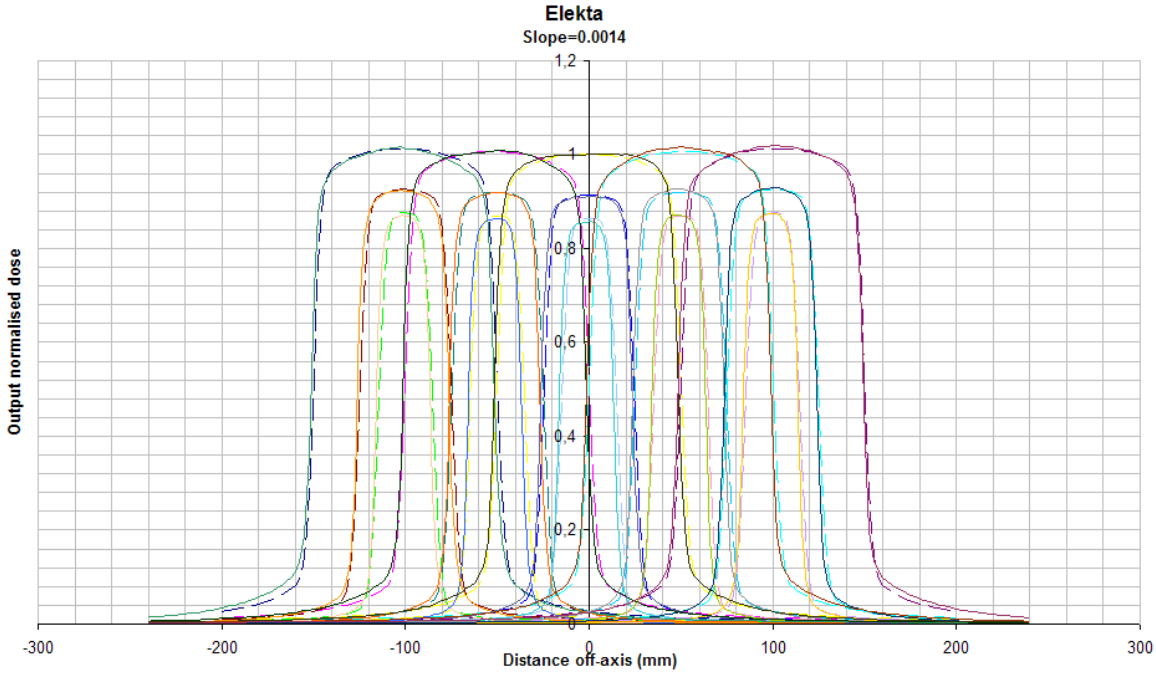

Figure 4.5 The fields for the Elekta accelerator with the slope fitted by the small fields. The calculated values are dashed lines.

The slopes found were smaller than the ones derived for the Varian accelerator; this is strictly due to the fact that they are two different machines and the head scatter and flattening filter shape differ. The slope derived from the larger field has a higher value in this case as well.

When using the lower value for the slope (Figure 4.5), good agreement was found and all average deviations were under 1%. The maximum deviations ranged from 0.59 % to 1.49 %. The deviations are presented in Table 4.8, in percentage.

Table 4.8 Deviations between RVP and the LDA for S=0.0014

Average deviation, 3x3	0.49
Average deviation, 5x5	0.82
Average deviation, 10x10	0.35
Average deviation, all fields	0.55
Minimum deviation	0.09
Average minimum deviation	0.20
Maximum deviation	1.49
Average maximum deviation	1.16

When the slope was raised to 0.0038, the slope derived form the 40x40 cm^2-field, RVP over calculated the dose, just as with the Varian. In this case RVP over-calculates at the off-axis point of 5 cm and continues to deviate for 10 cm (Figure 4.6).

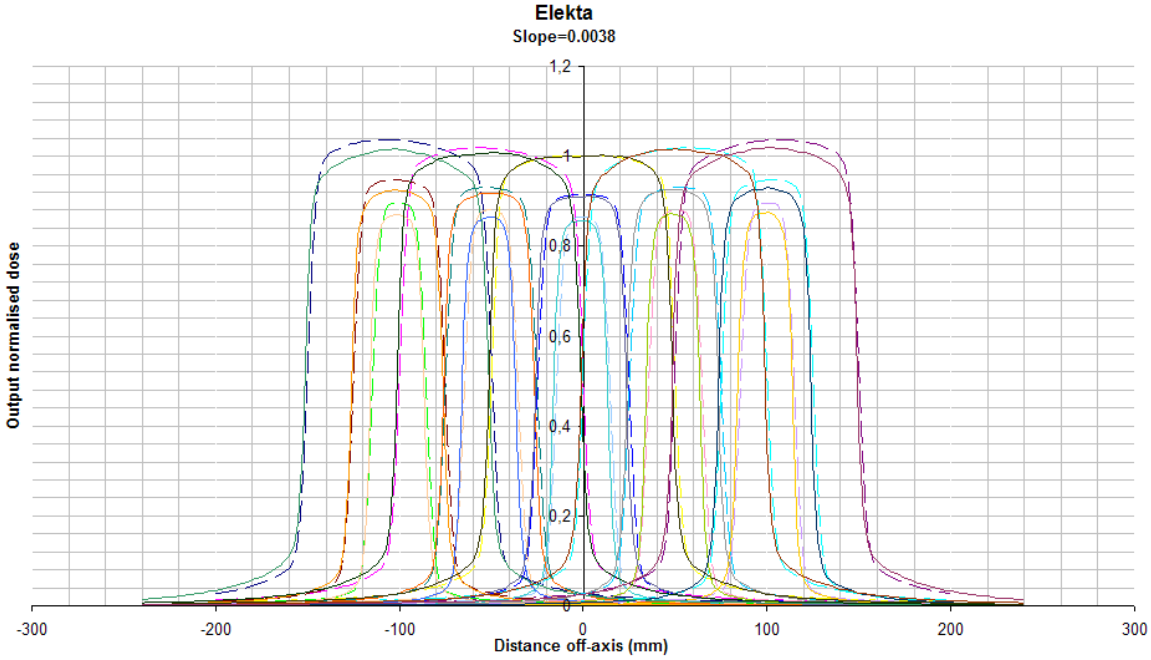

Figure 4.6 The fields for the Varian accelerator with the slope fitted by the large field. The calculated values are dashed lines.

Although the minimum deviations were low and the average deviations all were under 1.50%, the maximum deviations were large and the average maximum deviation was over 2%.

Table 4.9 Deviations between RVP and the LDA for S=0.0038

Average deviation, 3x3	1.09
Average deviation, 5x5	0.96
Average deviation, 10x10	1.36
Average deviation, all fields	1.14
Minimum deviation	0.004
Average minimum deviation	0.16
Maximum deviation	2.85
Average maximum deviation	2.31

It can also be seen that for both the Varian accelerator and the Elekta accelerator the leakage is under-estimated. There are also some discrepancies in the penumbra. Since one IMRT field is several segments placed on top of each other these effects could cancel each other out or enhance each other.

Different methods have been presented on how to deal with the off-axis dose changes. The off-axis softening, proposed by Tailor *et.al*. [1998], only deals with the effects of the flattening filter and does not account for the change in head scatter. However, this only accounts for the shape of the flattening filter and therefore does not fully compensate for the change in head scatter.

As for head scatter and off-axis dose modelling in general there have been many publications as well. Some of these model are complicated and/or do not agree with measurements and the aim of this project was to find a simple model to be used as a modification to an existing model. Other models have been presented by e.g. Hounsell and Wilkinson [1997], Loshek and Parker [1993] and Tsalafoutas *et.al.* [2003]. These models do give a good agreement between calculations and measurements but do approach the problem of off-axis dose increases in different ways than in this project. Hounsell and Wilkinson [1997] presented a model that was empirical. This model had good results but required a series of measurements to fit the parameters as well as newly constructed phantoms. The model by Tsalafoutas *et.al* [2003] uses many parameters, thus increasing the risk of errors. The model by Loshek and Parker [1993] uses accelerator specific parameters such as TMR (Tissue-to-Maximum Ratio) and SMR (Scatter-to-Maximum Ratio) and these must be gathered for off-axis distances as well. This model also uses several parameters.

The model presented in this project has few variable parameters that are obtained using few easy measurements with standard phantoms. This makes for a simple fast implementation of the off-axis dose calculation. The agreement found between the calculated and measured values, when using this model, was good. Therefore this method can be used for simpler calculations. The parameters, S, L and W, are set in the machine data file in RVP, for each accelerator and energy and are thereafter accounted for in all future calculations. This makes this model easy to implement once the measurements have been performed, evaluated and optimised. The slope derived from the largest field ($40\text{x}40\ \text{cm}^2$) could not be used. This was unfortunate, since the data for this field usually has been measured during commissioning and thus would not require any new measurements. However, since it was shown that this slope was not as good, the slope derived from the smaller fields must be used.

For profiles, this model does not show perfect agreement near the fields' edges. This could either be enhanced when calculating IMRT fields or the effect could cancel out. Therefore the model was also tested on IMRT fields to see what happens, enhancement or cancellation, and if this has major importance.

4.3 IMRT Measurements

The IMRT measurements were performed on the Elekta Precise with seven IMRT fields which together formed an entire treatment for tonsil cancer. The measured and calculated fields were evaluated in the IMRT verification programme Omnipro ImRT (Scanditronix-Wellhöfer) using gamma evaluation.

In Figure 4.7 the measured (top left) and the calculated (bottom left) matrices can be found. They are here at same resolution, of the same size and on the same scale. The resulting gamma matrix can also be seen (bottom right) as well as a profile through the y-axis at Y=0. The gamma evaluation has been performed over the entire field of view, not just over the irradiated part. The criteria for the gamma evaluation in the figure are 5%/5mm.

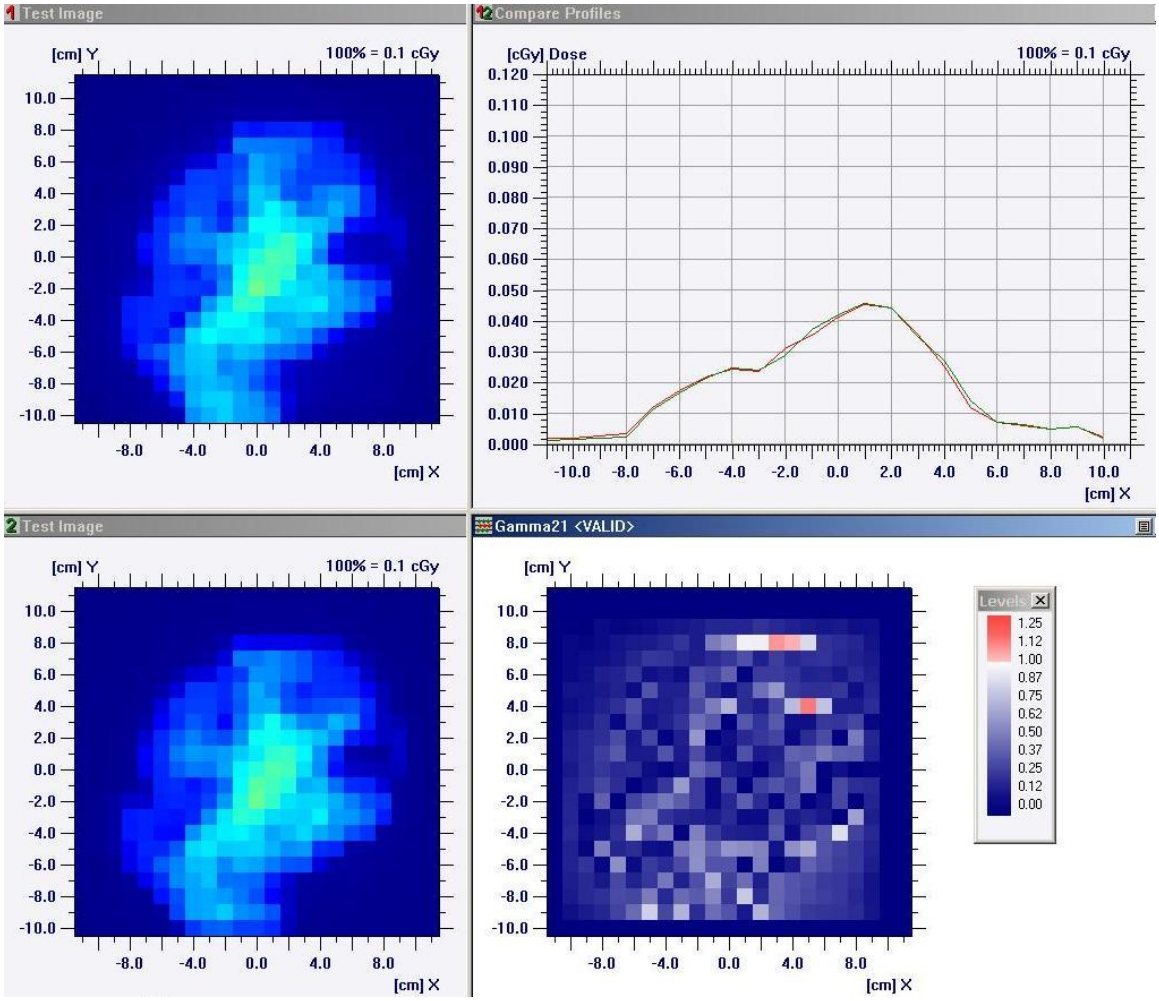

Figure 4.7 The matrices for field 2

Since the two left matrices are on the same scale they are easily compared. As can be seen, the maximum doses do agree as well as the spread of the field. In the profile it can be seen that there are some discrepancies but these are minor. However, once evaluating the matrices with gamma comparison, it can be seen that most discrepancies do pass the evaluation. The discrepancies that were found near the fields' edges do not enhance each other. There are a few points that do not pass the gamma evaluation, but the pass rate, presented below, is high.

The rest of the matrices, with the 5%/5mm criteria, can be found in Appendix 2.

The data from the gamma evaluation was analysed and the pass rate, i.e. the fraction of the calculation points that pass the gamma criteria, was found. Table 4.10 shows the pass rates for all the seven fields and for the two sets of criteria.

Table 4.10 Pass rates for the gamma evaluation.

	F1	**F2**	**F3**	**F4**	**F5**	**F6**	**F7**
2 %/2 mm	83	89	82	78	86	89	85
5 %/5 mm	99	99	99	98	99	100	99

When the typical acceptance for the TPS (2 %/2 mm) was used as criterion around 80 % of the points passed the calculation, which is not good enough to rely on. However, as this is a secondary test the 5 %/5 mm criterion is probably more reasonable. For the larger criterion the pass rates were all higher than 98 %, which should be satisfactory for a secondary test method. It should also be noted that the resolution for the matrices is one cm and the demands set in the gamma comparison are below that. The search distance however, is larger that one matrix element (15 mm) so that points within the same ixel does not get compared twice.

5 Conclusions

For this work improvements in the dose-calculating model for RVP has been developed, implemented and tested. The intention for this model was to deal with the effects of fields off-axis, due to change in head scatter and changes of the flattening filter. In order to make the software do proper calculations for fields that are off-axis and consequently IMRT fields, these effects are of importance.

After the model was developed and implemented into RVP, the parameters of it were fitted to measurements. When adjusting the parameters according to the slope derived from the small fields the agreement was good. However when the slope derived from the 40x40 cm^2 field was used, the agreement was not as good. Therefore if this model is to be used, a slope fitted by all the small fields must be used.

The agreement at the fields' edges was not in totally good. Even though the agreement for the leakage and the penumbra was good, with the leakage a slightly under-estimated by RVP, the combination of these two could lead to miss-calculations. If small miscalculations are made, they could enhance each other for IMRT fields when the segments are placed on top of each other. It was found that these effects were not significant for IMRT fields.

The model proposed and implemented is a simple model for the modelling of head scatter change across the field. The model has been tested on an actual IMRT treatment and with a 5 %/5 mm criteria good results were given compared to the measured 2D arrays. More tests need to be conducted to guarantee statistical certainty and if they show similar results, there is no doubt that the model can be used clinically as a secondary test of the dose, even in IMRT cases.

6 Acknowledgements

First and foremost I would like to thank my supervisors, Dr. Sven Bäck and Dr. Crister Ceberg for taking their time to help me with this project.

Fredrik Nordström also deserves a special thank you for helping me with any RVP related problem and the measurements. I would also like to thank the rest of the staff at the radiotherapy departments of Lund and Malmö University Hospitals for help with anything I might have needed and also for creating a pleasant work atmosphere.

I would also like to thank my classmates. You have really made these past four and a half years to something memorable and I will look back with many fond memories.

I would also like to thank the people who have kept my mind off this work when I have needed it the most; my family, my friends and last but not least Martin. I sincerely thank you all!

7 Summary for the general public (in Swedish)

EN METOD FÖR ATT LÄTTARE BERÄKNA STRÅLDOSER TILL PATIENTER

Varje år får cirka 50 000 svenskar diagnosen cancer. Mot detta är strålbehandling en vanlig behandlingsmetod och det uppskattas att cirka en tredjedel av alla som får cancer någon gång under sin behandling får strålbehandling.

En viktig sak inom strålbehandling är att patienten får den dos som läkaren har ordinerat. Detta är en så vital detalj inom strålbehandling att SSI, Statens Strålskyddsinstitut, har reglerat att dosen ska beräknas med två oberoende metoder innan behandling. Detta för att kunna säkerställa patientdosen.

Vid de båda universitetssjukhusen i Lund och Malmö har man tidigare utvecklat ett datorprogram som gör just detta, beräknar dosen med en oberoende metod. Detta program är fortfarande under utveckling, men används också kliniskt för beräkningar av doser vid enkla behandlingar.

Ett strålfält från en linjäraccelerator är inte homogent. Mitt i fältet, i isocenter, är den plats som alla data finns om. Eftersom fältet ändras blir dosen olika vid olika platser i fältet och det finns ingen generell metod för hur dosen ändras, detta är individuellt för alla linjäracceleratorer.

I detta projekt har en metod utvecklas som tar hänsyn till dessa förändringar på ett enkelt sätt. På så sätt kan man verkligen vara säker på att datorprogrammet räknar rätt och på så sätt kan man verifiera att patienten får rätt stråldos vid sin strålbehandling.

Modellen testades först för profiler genom strålfältet vilket visade sig ge en bra överrensstämmelse. Vidare testades modellen också för fält som används vid patientbehandlingar. Dessa fält är intensitetsmodulerade vilket innebär att många fält placeras ovanpå varandra. I och med detta skulle ett litet fel kunna fortplantas och ge ett stort totalt fel. Då modellen testades gavs inga stora avvikelser. Emellertid testades inte tillräckligt många fält för att kunna garantera statistik säkerhet, men visar ytterligare test på samma resultat skulle modellen kunna användas i kliniken för beräkningar av stråldoser till patienter.

8 References

8.1 Articles

Bjärngard, B.E., Shackford, H. 1994. Attenuation in high energy x-ray beams, *Medical Physics* 21. 1069-1073

Bjärngard, B.E., Vadash, P., 1995 Analysis of central-axis doses for high-energy X-rays. *Medical Physics* 22, 1191-1195

Bortfeld, T. 2006, IMRT: A Review and Preview. *Physics in Medicine and Biology* 51, 363-379

Carlson, D., 2001, Intensity Modulation Using Multileaf Collimators: Current Status, *Medical Dosimetry* 26, 151-156

Dosimetry Phantoms, Solid Water™ Phantom Materials.
http://www.cnmcco.com/images/Solid%20Water.pdf

Hannallah, D., Zhu, T.C., Bjärngard, B.E., 1996, Electron disequilibrium in high-energy x-ray beams. *Medical Physics* 23, 1867-1871

Hounsell, A.R., Wilkinson, J.M., 1997, Head scatter modelling for irregular field shaping and beam intensity modulation, *Physics of Medicine and Biology* 42, 1737-1749

IAEA Report; *Quality Assurance of External Beam Radiotherapy*
http://www-naweb.iaea.org/nahu/dmrp/pdf_files/Chapter12.pdf

IAEA report TRS-398.
http://www-naweb.iaea.org/nahu/dmrp/pdf_files/CoPV11b.pdf#search=%22TRS-398%22

ICRP Report *Radiation and Your Patient: A Guide For Medical Practitioners*
http://www.icrp.org/docs/Rad_for_GP_for_web.pdf

Johnsson, S. 2003 Development and Evaluation of an Independent System for Absorbed Dose Calculations in Radiotherapy, Lund University (Ph.D. Thesis), Department of Radiation Physics, The Jubileum Institute, Lund University, 91-628-5498-4

Johnsson, S.A., Ceberg, C.P., Knöös, T., Nilsson, P., 1999. Transmission measurements in air using the ESTRO mini-phantom. *Physics of medicine and biology* 44, 2445-2450.

Knöös, T., Ceberg, C., Weber, L., Nilsson, P. 1994. The dosimetric verification of a pencil beam based treatment planning system. *Physics of medicine and biology* 39. 1609-1628

Knöös, T, Johnsson, SA., Ceberg, C.P., Tomaszewicz, A., Nilsson, P., 2001, Independent checking of the delivered dose for high-energy X-rays using a hand-held PC. *Radiotherapy and Oncology* 58, 201-208

Loshek, D.D., Parker, T.T., 1993, Dose calculation in static or dynamic off-axis fields *Medical Physics* 21, 401-410

Low, D.A., Harms, W.B., Mutic, S., Purdy, J.A. 1998 A technique for the quantitative evaluation of dose distributions. *Medical Physics* 25, 656-661

Metcalfe, P., Kron, T., Hoban, P. 1997. *The Physics of Radiotherapy X-Rays from Linear Accelerators*. Madison, WI. Medical Physics Publishing. 0-944838-76-6

Nordström, F., Björk, P., Bäck, S., Ceberg, C., Holmberg, O., Johnsson, S., 2006 Implementation of an Independent Calculation Method for Verification of Monitor Units and Dose Distribution in IMRT, *ESTRO 25 (Poster Abstract)*

OmniPro ImRT System Manual, Scanditronix Wellhöfer

OncoLog, IMRTlog technical information
http://www.oncolog.net/web/oncWeb.nsf/webfiles/IMRTTechnicalDesc.pdf/$file/IMRT_T0605a.pdf

Scanditronix-Wellhöfer webpage,
http://www.scanditronix-wellhofer.com/

SOS; Sweden's National Board of Health and Welfare, Statistics,
http://www.socialstyrelsen.se/Statistik/statistikdatabas/ (In Swedish)

SSI constitution 2000:1; *Regulations on General Obligations in Medical and Dental Practices using Ionising Radiation*
http://www.ssi.se/forfattning/PDF_Eng/2000-1e.PDF

SSI constitution 2000:4; *Regulations on Radiation Therapy*.
http://www.ssi.se/forfattning/PDF_Eng/2000-1e.PDF

Svensson, H., Möller, TR. 2003 Developments in Radiotherapy. *Acta Oncologica* 42, 430-442

Tailor, R.C., Tello, V.M., Schroy, C.B., Vossler, M., Hanson, W.F., 1998. A generic off-axis energy correction for linac photon beam dosimetry. *Medical Physics* 25, 662-667

Tsalafoutas, I.A., Xenofos, S., Yakoumakis, E., Nikoletopoulos, S., 2003. A Semiempirical method for the description of off-center rations at depth from linear accelerators. *Medical Dosimetry* 28, 119-125

The Swedish Cancer Society
www.cancerfonden.se

Xiao, Y., Bjärngard, BE., Reiff, J., 1999, Equivalent fields and scatter integration for photon fields. *Physics of Medicine and Biology* 44, 1053-1065

9 Appendices

9.1 Appendix 1, List of Abbreviations

ADC	Analogue to Digital Converter
CT	Computer Tomography
IAEA	International Atomic Energy Agency
ICRP	International Commission of Radiological Protection
IMRT	Intensity Modulated Radiation Therapy
KERMA	Kinetic Energy Released by Ionising Radiation in Matter
LDA	Linear Diode Array
MLC	Multi Leaf Collimator
MRI	Magnetic Resonance Imaging
MU	Monitor Unit
MV	Mega Voltage
PET	Positron Emission Tomography
RVP	Radiation Verification Programme
SMR	Scatter-to-maximum ratio
SSD	Source Surface Distance
SSI	The Swedish Radiation Protection Authority
TMR	Tissue-to-maximum ratio
TPS	Treatment Planning System

9.2 Appendix 2 LDA measurements for Varian accelerator

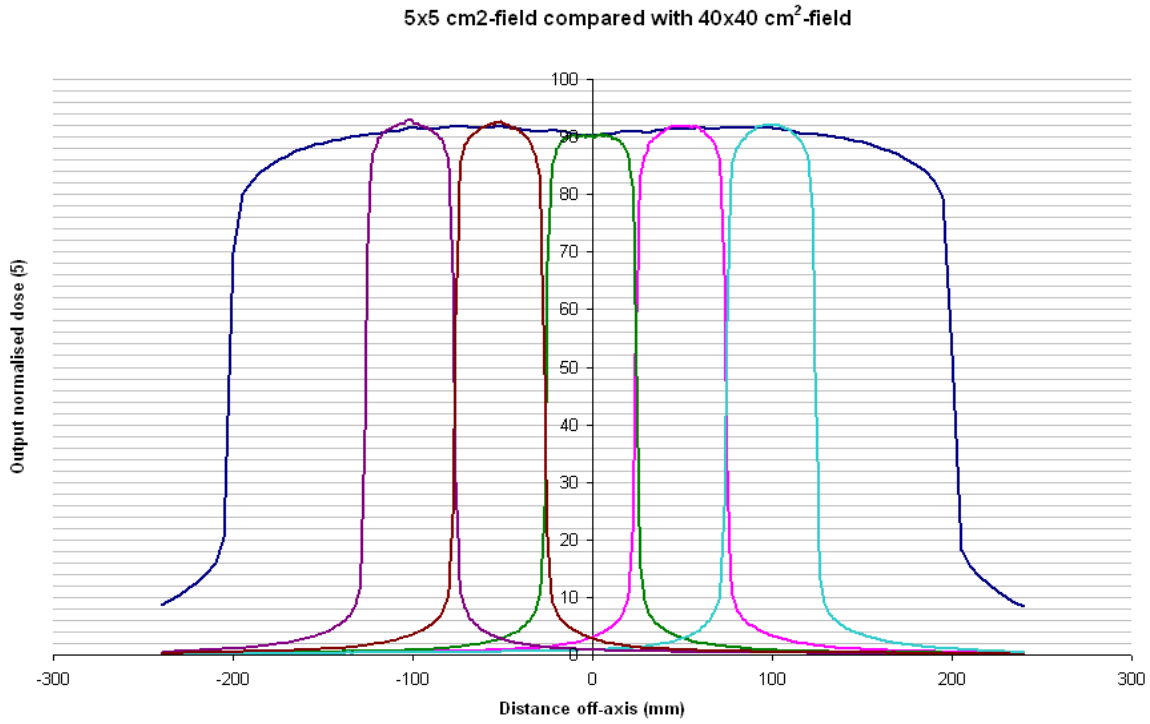

The 5x5 cm^2 fields overlapped with the 40x40 cm^2 field for the Varian accelerator

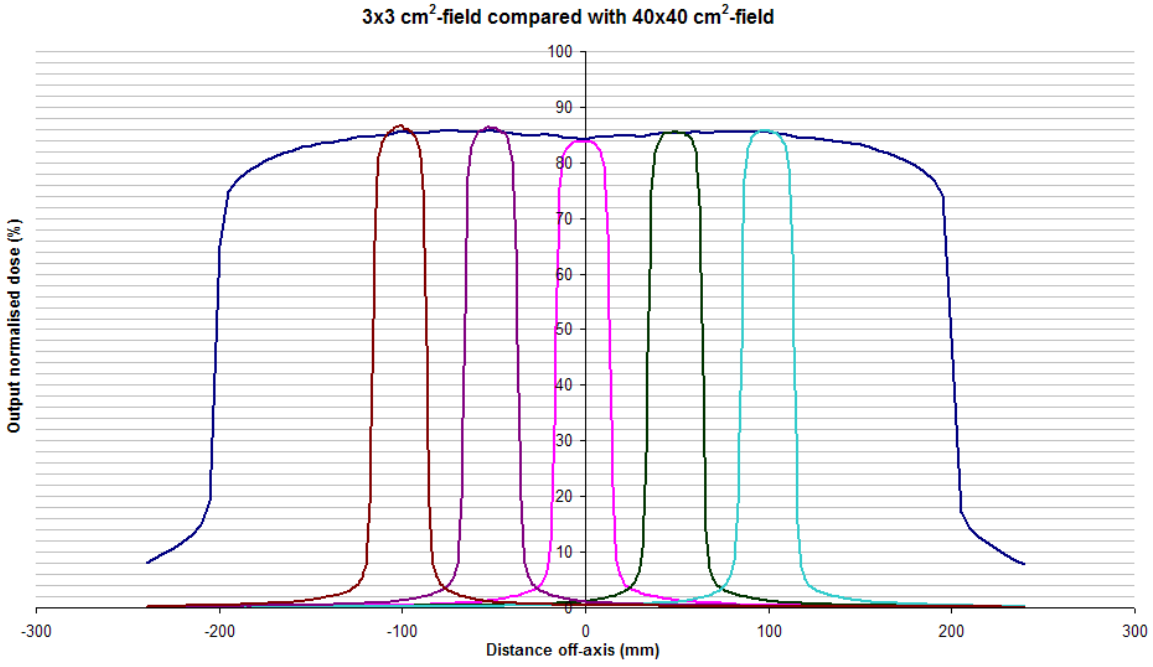

The 3x3 cm^2 fields overlapped with the 40x40 cm^2 field for the Varian accelerator

9.3 Appendix 3 LDA measurements for Elekta accelerator

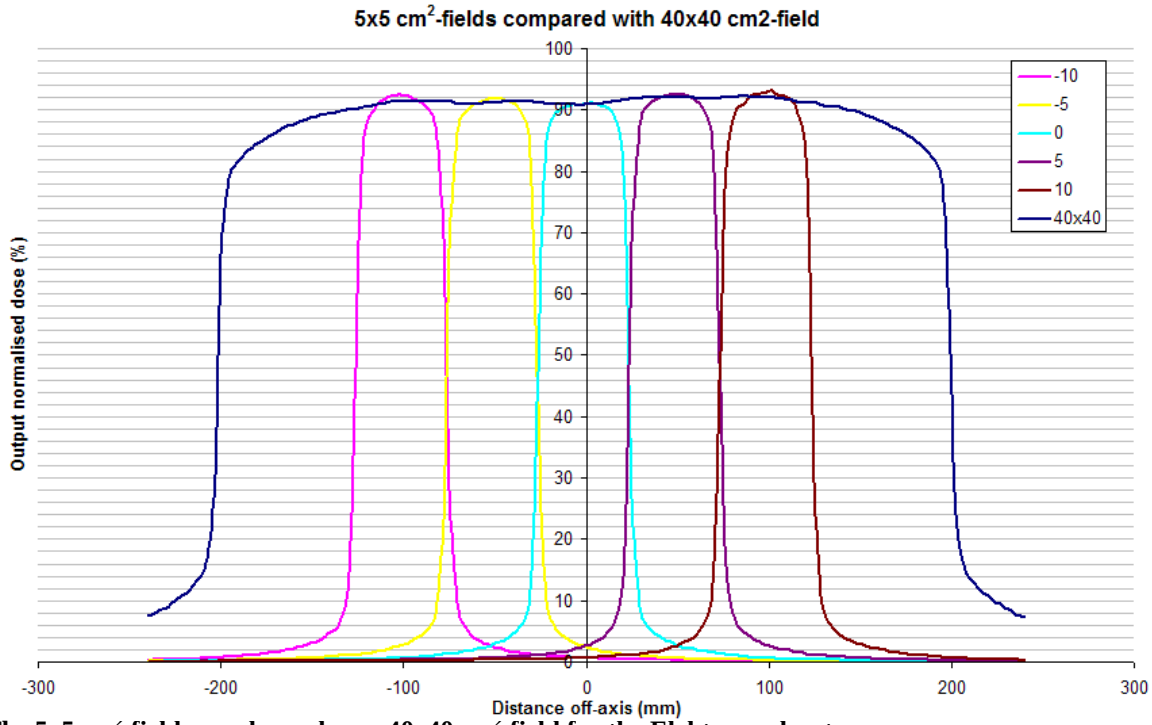

The 5x5 cm^2 fields overlapped on a 40x40 cm^2 field for the Elekta accelerator

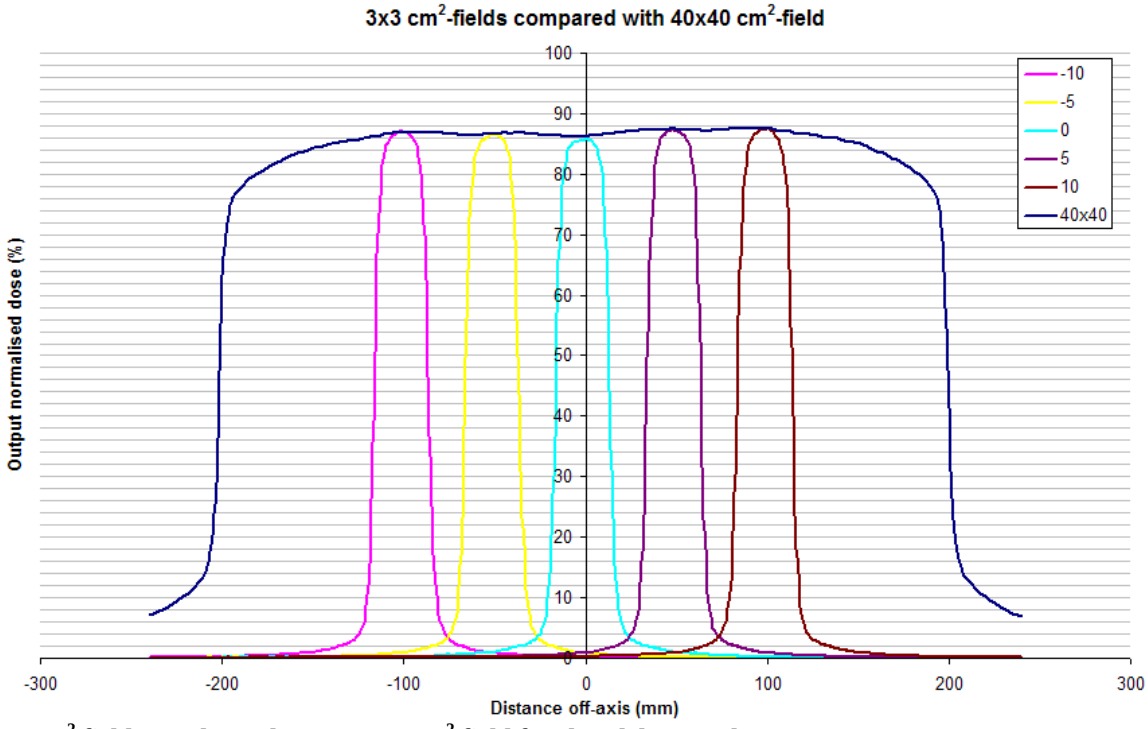

The 3x3 cm^2 fields overlapped on a 40x40 cm^2 field for the Elekta accelerator

9.4 Appendix 4, Calculated, Measured and Gamma Matrices

All of these images are built up in the same way;
Top left: Measured matrix
Bottom left: Calculated matrix
Top right: Profile view at y=0 (red line=measured, green line=calculated)
Bottom right: Quotient, calculated vs. measured.

Field 1 (Gamma data has gone missing)

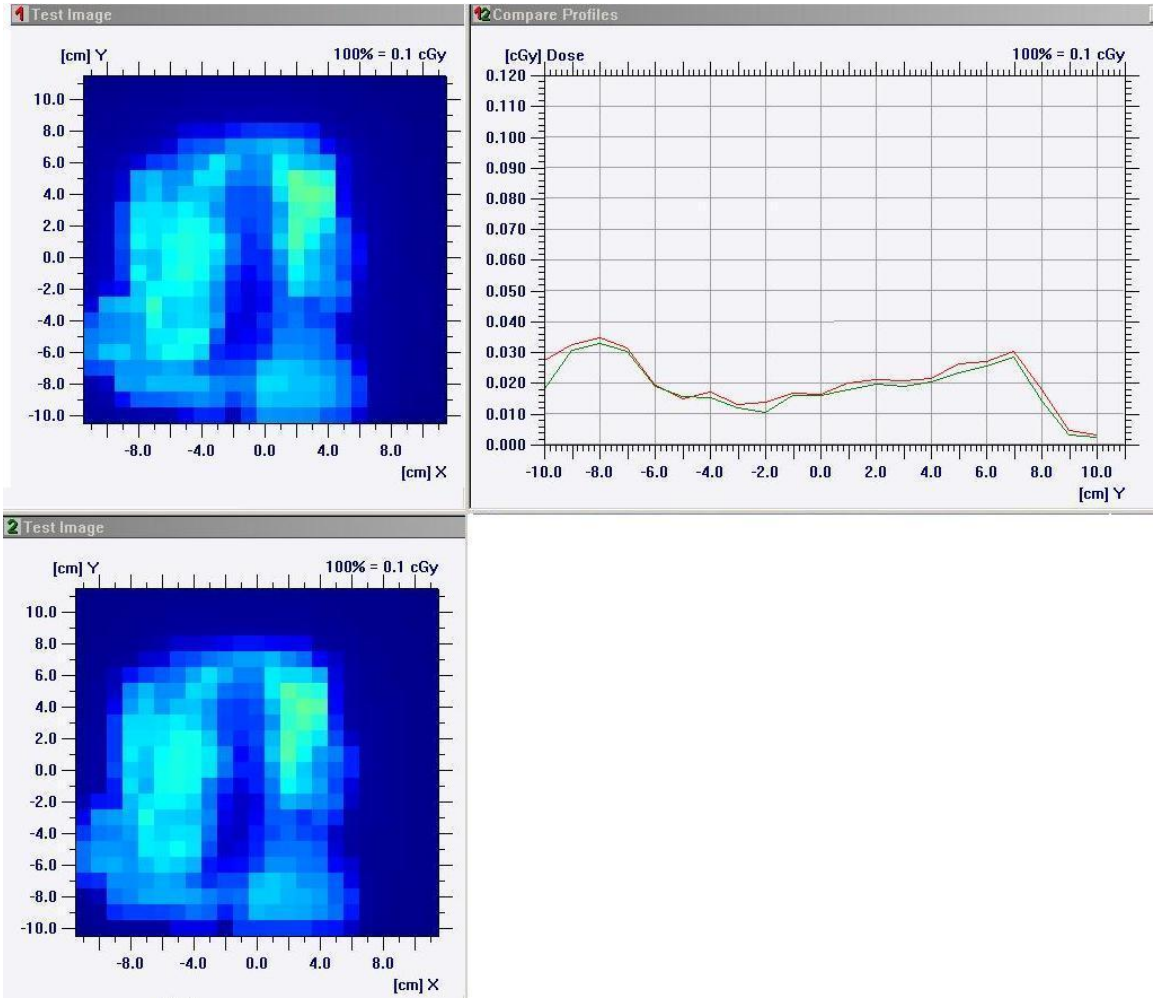

Field 3

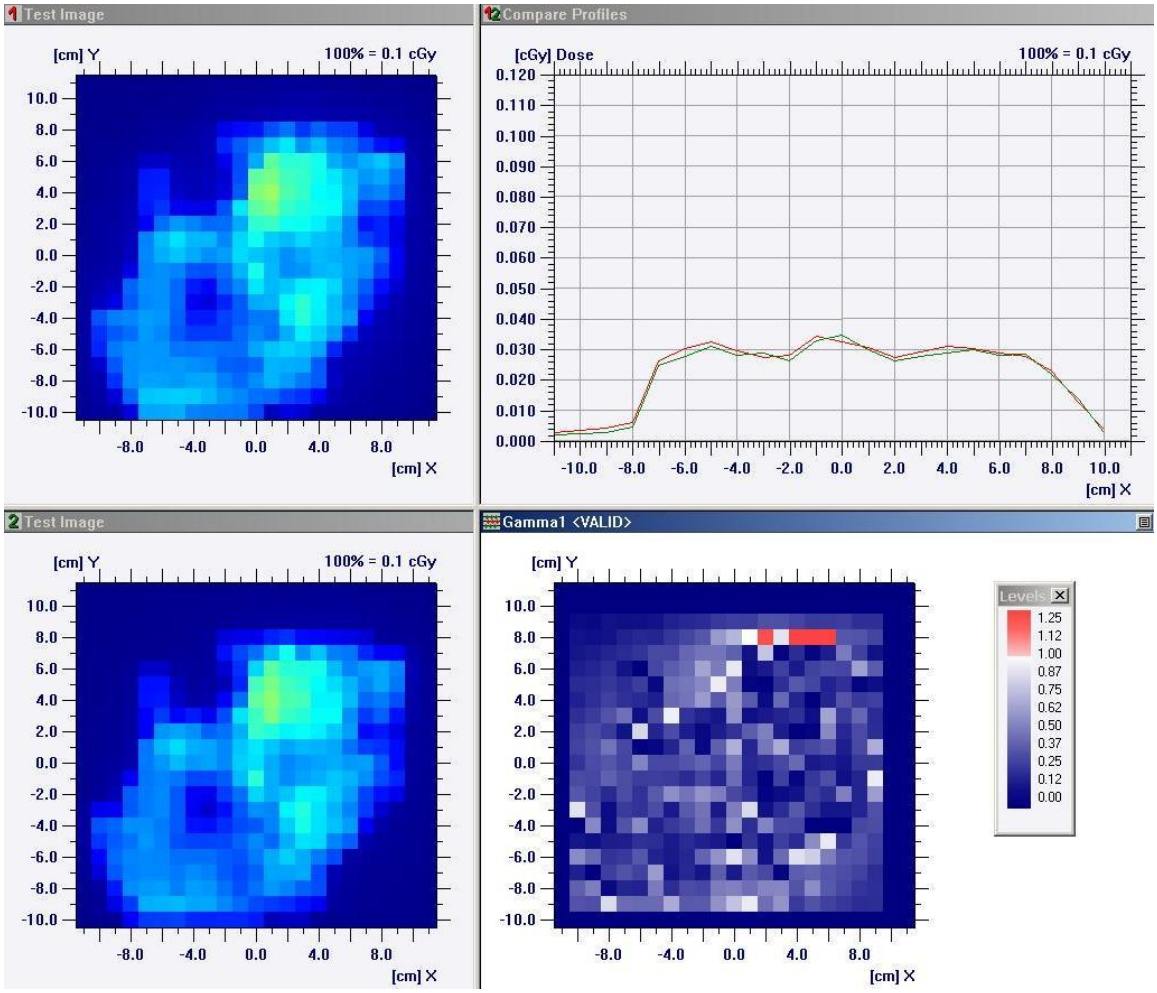
Test Image
[cm] Y
100% = 0.1 cGy
10.0
8.0
6.0
4.0
2.0
0.0
-2.0
-4.0
-6.0
-8.0
-10.0
-8.0
-4.0
0.0
4.0
8.0
[cm] X
Compare Profiles
[cGy] Dose
100% = 0.1 cGy
0.120
0.110
0.100
0.090
0.080
0.070
0.060
0.050
0.040
0.030
0.020
0.010
0.000
-10.0
-8.0
-6.0
-4.0
-2.0
0.0
2.0
4.0
6.0
8.0
10.0
[cm] X
Test Image
[cm] Y
100% = 0.1 cGy
[cm] X
Gamma1 <VALID>
[cm] Y
Levels
1.25
1.12
1.00
0.87
0.75
0.62
0.50
0.37
0.25
0.12
0.00
[cm] X

Field 4

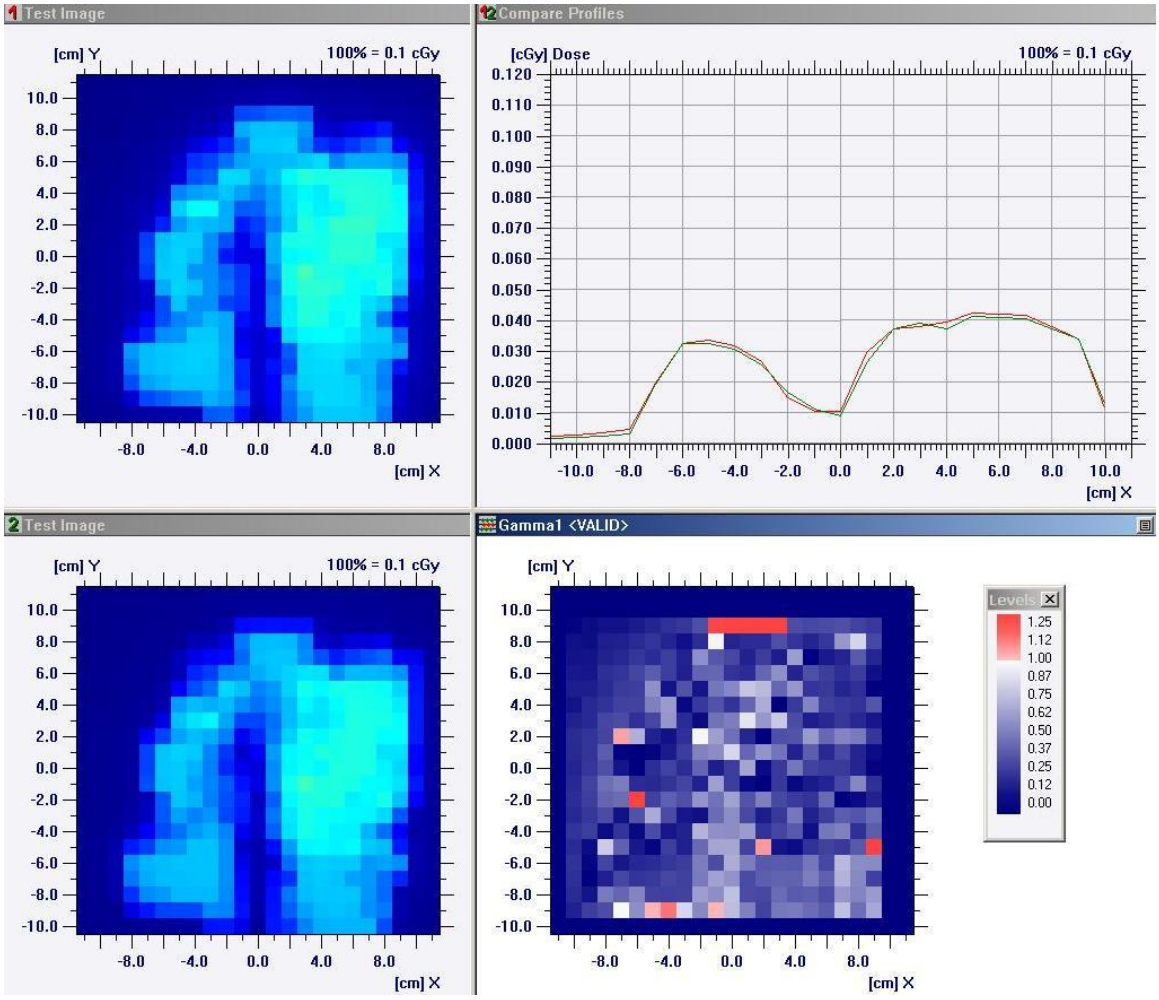
Test Image
[cm] Y
100% = 0.1 cGy
10.0
8.0
6.0
4.0
2.0
0.0
-2.0
-4.0
-6.0
-8.0
-10.0
-8.0
-4.0
0.0
4.0
8.0
[cm] X
Compare Profiles
[cGy] Dose
100% = 0.1 cGy
0.120
0.110
0.100
0.090
0.080
0.070
0.060
0.050
0.040
0.030
0.020
0.010
0.000
-10.0
-8.0
-6.0
-4.0
-2.0
0.0
2.0
4.0
6.0
8.0
10.0
[cm] X
Test Image
[cm] Y
100% = 0.1 cGy
[cm] X
Gamma1 <VALID>
[cm] Y
Levels
1.25
1.12
1.00
0.87
0.75
0.62
0.50
0.37
0.25
0.12
0.00
[cm] X

Field 5

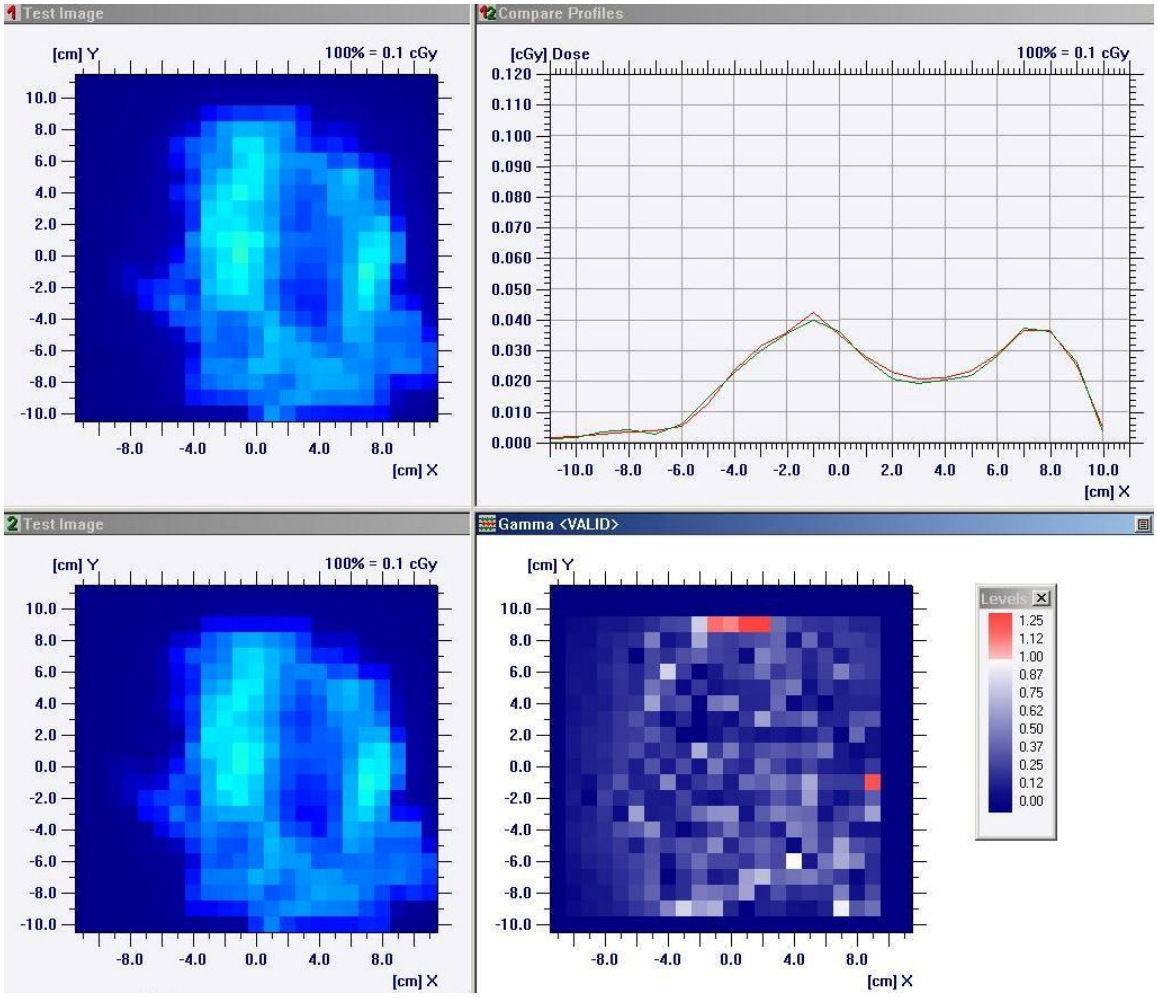
Test Image
[cm] Y
100% = 0.1 cGy
10.0
8.0
6.0
4.0
2.0
0.0
-2.0
-4.0
-6.0
-8.0
-10.0
-8.0
-4.0
0.0
4.0
8.0
[cm] X
Compare Profiles
[cGy] Dose
100% = 0.1 cGy
0.120
0.110
0.100
0.090
0.080
0.070
0.060
0.050
0.040
0.030
0.020
0.010
0.000
-10.0
-8.0
-6.0
-4.0
-2.0
0.0
2.0
4.0
6.0
8.0
10.0
[cm] X
Test Image
[cm] Y
100% = 0.1 cGy
[cm] X
Gamma <VALID>
[cm] Y
Levels
1.25
1.12
1.00
0.87
0.75
0.62
0.50
0.37
0.25
0.12
0.00
[cm] X

Field 6

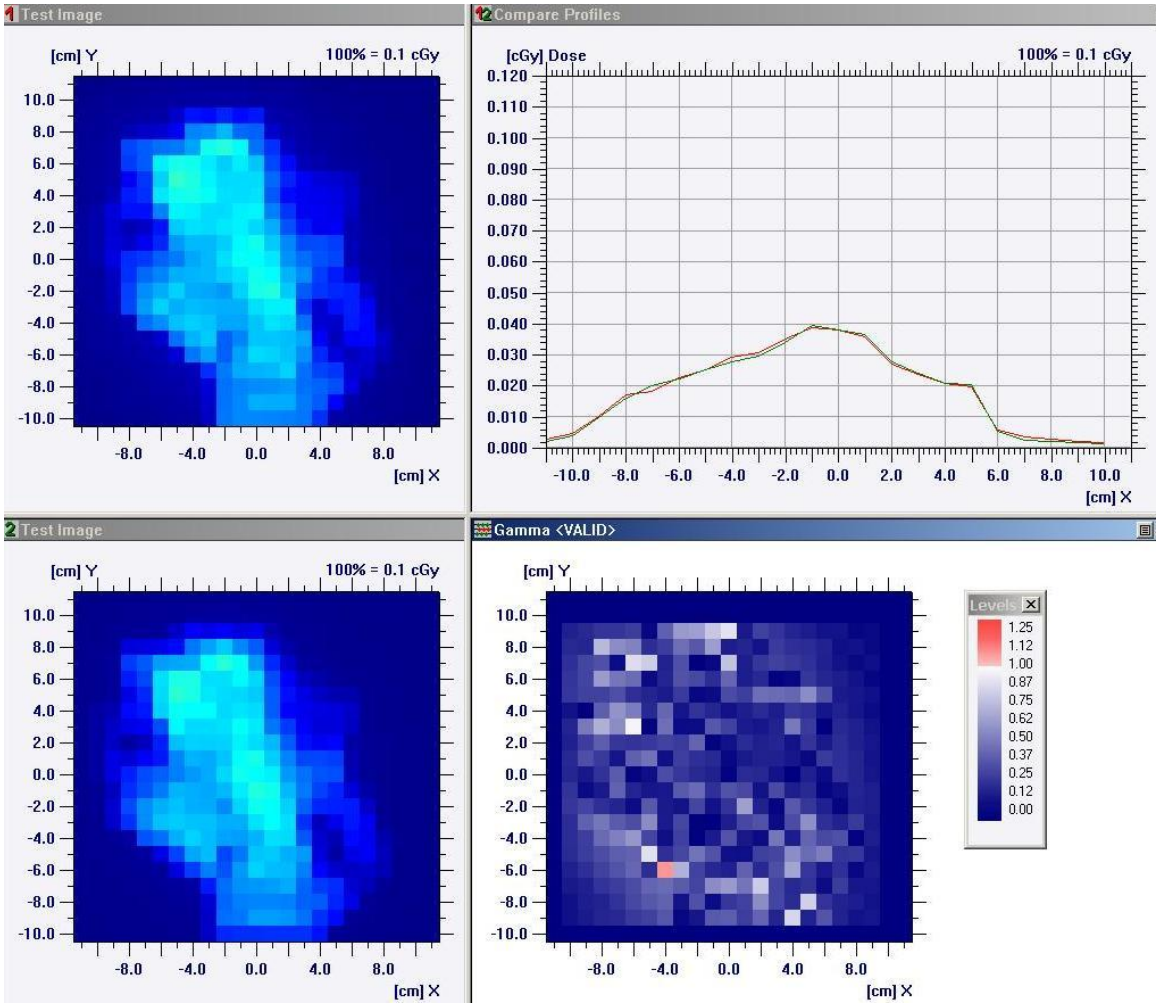
Test Image
[cm] Y
100% = 0.1 cGy
10.0
8.0
6.0
4.0
2.0
0.0
-2.0
-4.0
-6.0
-8.0
-10.0
-8.0
-4.0
0.0
4.0
8.0
[cm] X
Compare Profiles
[cGy] Dose
100% = 0.1 cGy
0.120
0.110
0.100
0.090
0.080
0.070
0.060
0.050
0.040
0.030
0.020
0.010
0.000
-10.0
-8.0
-6.0
-4.0
-2.0
0.0
2.0
4.0
6.0
8.0
10.0
[cm] X
Test Image
[cm] Y
100% = 0.1 cGy
[cm] X
Gamma <VALID>
[cm] Y
Levels
1.25
1.12
1.00
0.87
0.75
0.62
0.50
0.37
0.25
0.12
0.00
[cm] X

Field 7

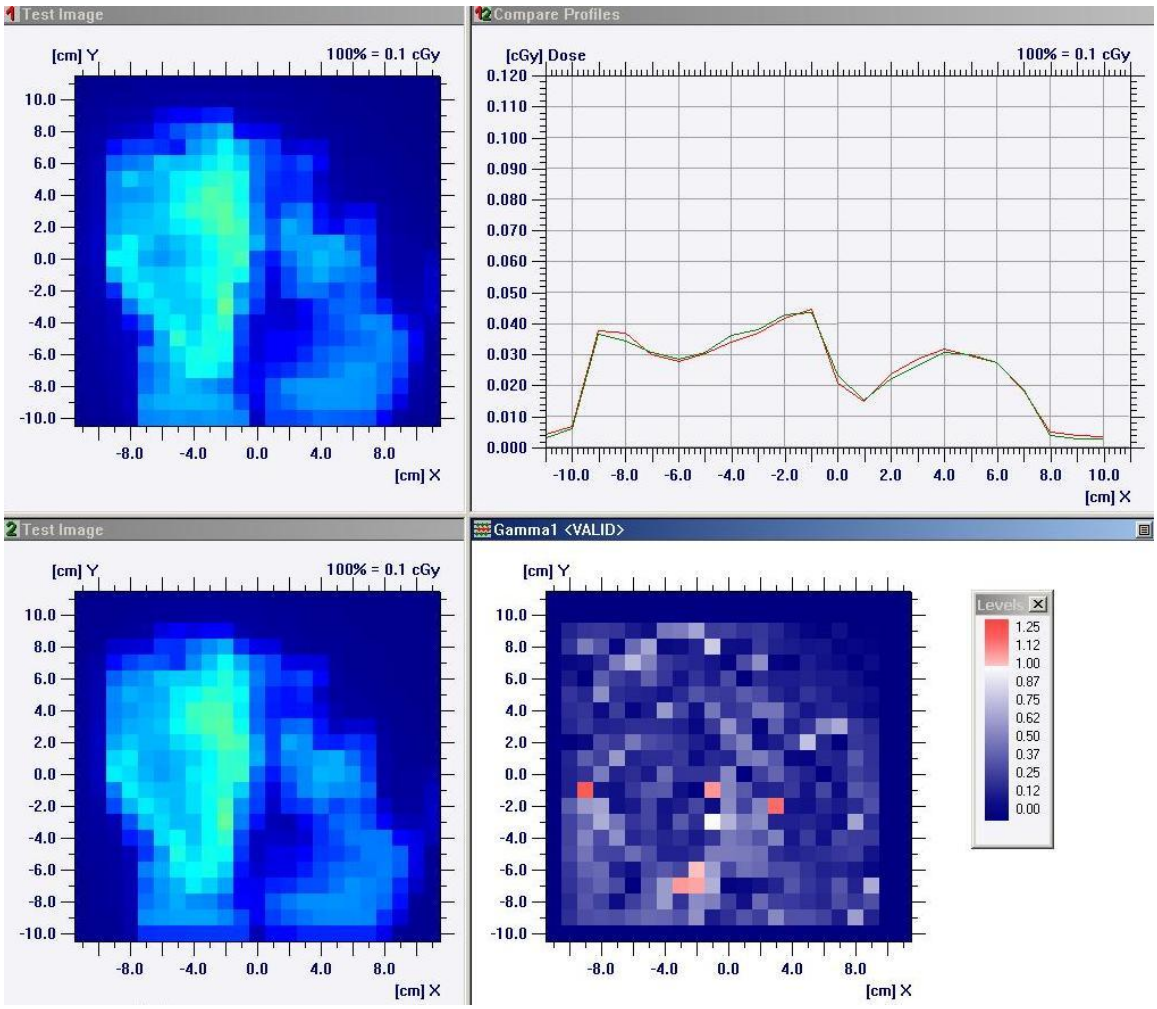
Test Image
[cm] Y
100% = 0.1 cGy
10.0
8.0
6.0
4.0
2.0
0.0
-2.0
-4.0
-6.0
-8.0
-10.0
-8.0
-4.0
0.0
4.0
8.0
[cm] X
Compare Profiles
[cGy] Dose
100% = 0.1 cGy
0.120
0.110
0.100
0.090
0.080
0.070
0.060
0.050
0.040
0.030
0.020
0.010
0.000
-10.0
-8.0
-6.0
-4.0
-2.0
0.0
2.0
4.0
6.0
8.0
10.0
[cm] X
Test Image
[cm] Y
100% = 0.1 cGy
[cm] X
Gamma1 <VALID>
[cm] Y
Levels
1.25
1.12
1.00
0.87
0.75
0.62
0.50
0.37
0.25
0.12
0.00
[cm] X